Three methionine residues located within the regulator of conductance for K^+ (RCK) domains confer oxidative sensitivity to large-conductance Ca^{2+}-activated K^+ channels

Lindsey Ciali Santarelli[1,2], Ramez Wassef[1], Stefan H. Heinemann[3] and Toshinori Hoshi[1,2]

[1] *Department of Physiology and* [2] *Neuroscience Graduate Group, University of Pennsylvania, 3700 Hamilton Walk, Philadelphia, Pennsylvania 19104, USA*

[3] *Molecular and Cellular Biophysics, Medical Faculty of the Friedrich Schiller University Jena, Drackendorfer Strasse 1, D-07747 Jena, Germany*

Methionine-directed oxidation of the human Slo1 potassium channel (hSlo1) shifts the half-activation voltage by −30 mV and markedly slows channel deactivation at low concentrations of intracellular Ca^{2+} ($[Ca^{2+}]_i$). We demonstrate here that the contemporaneous mutation of M536, M712 and M739 to leucine renders the channel functionally insensitive to methionine oxidation caused by the oxidant chloramine-T (Ch-T) without altering other functional characteristics. Coexpression with the auxiliary β1 subunit fails to restore the full oxidative sensitivity to this triple mutant channel. The Ch-T effect is mediated specifically by M536, M712 and M739 because even small changes in this residue combination interfere with the ability to remove the oxidant sensitivity following mutation. Replacement of M712 or M739, but not M536, with the hydrophilic residue glutamate largely mimics oxidation of the channel and essentially removes the Ch-T sensitivity, suggesting that M712 and M739 may be part of a hydrophobic pocket disrupted by oxidation of non-polar methionine to the more hydrophilic methionine sulfoxide. The increase in wild-type hSlo1 open probability caused by methionine oxidation disappears at high $[Ca^{2+}]_i$ and biophysical modelling of the Ch-T effect on steady-state activation implicates a decrease in the allosteric coupling between Ca^{2+} binding and the pore. The dramatic increase in open probability at low $[Ca^{2+}]_i$ especially within the physiological voltage range suggests that oxidation of M536, M712 or M739 may enhance the Slo1 BK activity during conditions of oxidative stress, such as those associated with ischaemia-reperfusion and neurodegenerative disease, or in response to metabolic cues.

(Received 2 November 2005; accepted after revision 27 December 2005; first published online 5 January 2006)
Corresponding author T. Hoshi: Department of Physiology, University of Pennsylvania, 3700 Hamilton Walk, Philadelphia, PA 19104–6085, USA. Email: hoshi@hoshi.org

Oxidants generated by cellular metabolism are implicated in normal cellular signalling as well as the pathogenesis of many diseases, such as neurodegenerative diseases and various vascular disorders. While the reactive oxidants alter many cellular constituents, amino acids in proteins are the prime target for oxidative modification. The amino acid methionine is particularly susceptible to oxidation due to the presence of a highly reactive sulphur atom within its hydrophobic but yet flexible side chain. Upon oxidation by either endogenous species (e.g. H_2O_2, hydroxyl radical, chloramines) or exogenous reagents (e.g. chloramine-T, dimethyl sulfoxide), methionine is oxidized to methionine sulfoxide (met-O). The more hydrophilic and less flexible side chain of met-O can readily alter the secondary structure of a protein (Stadtman *et al.* 2003; Weissbach *et al.* 2005). For instance, if a given methionine residue is clustered with other hydrophobic residues in a 'pocket', then oxidation to the more hydrophilic met-O may cause the pocket to open or change shape (Vogt, 1995). In fact, the hydrophobicity index of met-O is comparable to that of the hydrophilic residues asparagine, glutamine and lysine (Black & Mould, 1991).

The chemical and physical changes caused by methionine oxidation drastically alter the functions of many biological molecules, including α1-proteinase inhibitor in the lung (Johnson & Travis, 1979; Evans & Pryor, 1994), selected hormones (Houghten & Li, 1976; Teh *et al.* 1987; Zull *et al.* 1990), *Shaker* potassium channels (Ciorba *et al.* 1997, 1999; Chen *et al.* 2000), and calmodulin (Gao *et al.* 1998). The reversibility

 DOI: 10.1113/jphysiol.2005.101089

of the methionine–met-O reaction enabled by the methionine sulfoxide reductases (MSRs), as exemplified by reactivation of the plasma membrane Ca-ATPase system following MSR-mediated reduction of calmodulin (Sun *et al.* 1999), suggests that modification of methionine residues may be an important and prevalent component in signal transduction and the antioxidant system (Levine *et al.* 1996). Consistent with the idea, increased levels of amino acid oxidation caused by a genetic disruption of the MSR system lead to cerebellar dysfunction and shortened lifespan in mice (Moskovitz *et al.* 2001).

Another important cellular protein subject to methionine oxidation is the large-conductance calcium- and voltage-gated BK channel (Tang *et al.* 2001; Santarelli *et al.* 2004). The opening of BK channels significantly impacts on the cellular resting membrane potential because of their large unitary conductance. The net efflux of potassium ions through BK channels mediates crucial physiological functions, such as smooth muscle vaso-relaxation (Nelson *et al.* 1995; Brenner *et al.* 2000; Jaggar *et al.* 2000), repolarization and the after-hyperpolarization following an action potential in specific neurones (Storm, 1987; Zhang & McBain, 1995; Shao *et al.* 1999), and neurotransmitter release (Hu *et al.* 2001). Accordingly, BK channel expression is enriched in the brain and vascular smooth muscle. In heart muscle, BK channels located within mitochondria may be important for preconditioning the heart against ischaemic damage (Xu *et al.* 2002). Indeed, activation of the BK channel, mediated perhaps by oxidative modification, may serve a protective role in many physiological systems. In agreement with the wide distribution of BK channels, the absence of the gene encoding the pore-forming α subunit (Slo1) leads to a variety of adverse phenotypes, including elevated blood pressure (Sausbier *et al.* 2005) and cerebellar, urinary and erectile dysfunction (Meredith *et al.* 2004; Sausbier *et al.* 2004; Werner *et al.* 2005).

The Slo1 subunit contains seven putative transmembrane-spanning helical segments such that the S0 segment, which is considered to be the main site of Slo1 association with auxiliary β subunits (Wallner *et al.* 1996; Meera *et al.* 1997), places the amino terminus of the α subunit into the extracellular milieu. The extensive intracellular carboxyl terminus, constituting ~70% of the protein, probably provides contact sites for various modulators of the channel function and contains two probable RCK (regulator of conductance for K^+) domains (Jiang *et al.* 2002; Roosild *et al.* 2004). Three distinct sites within the RCK domains mediate the overall divalent cation sensitivity of the channel (Zeng *et al.* 2005). Analogous to the mechanism proposed to explain Ca^{2+}-dependent activation of the bacterial MthK channel (Jiang *et al.* 2002), the binding of Ca^{2+} to the Slo1 channel is postulated to result in expansion of the gating ring formed by the RCK domains and subsequent opening of the pore (Niu & Magleby, 2002). The energy transduction process mediated by the gating-ring complex contributes to the allosteric activation of the Slo1 channel (Horrigan *et al.* 1999; Rothberg & Magleby, 2000; Horrigan & Aldrich, 2002) and may serve as a primary effector for the numerous modulatory agents (e.g. Horrigan *et al.* 2005).

Methionine oxidation promoted by the biologically relevant oxidant chloramine-T reliably increases the steady-state activation of the human Slo1 (hSlo1) channel and slows channel deactivation in the virtual absence of Ca^{2+} in isolated excised patches (Tang *et al.* 2001; Santarelli *et al.* 2004). The functional effects of methionine oxidation are enhanced by the presence of the auxiliary β1 subunit, but modification of methionine residues within β1 is not responsible for the greater leftward shift of the *G–V* curve or the dramatic slowing of deactivation (Santarelli *et al.* 2004). These results suggest that the methionine residues modified to cause the characteristic functional changes, though unidentified, reside within the hSlo1 α subunit (Tang *et al.* 2001; Santarelli *et al.* 2004). Here, we show that M536, M712 and M739 located within the hSlo1 RCK domains confer methionine oxidative sensitivity to the channel. When all three residues are conservatively mutated to leucine, the channel fails to exhibit the typical electrophysiological consequences of the oxidative modification. Other functional properties of the triple mutant channel, such as Ca^{2+} sensitivity, are not altered by the mutations. Furthermore, the Ca^{2+} dependence of the oxidative effects in wild-type hSlo1 suggests that oxidation of the critical methionine residues diminishes allosteric coupling between Ca^{2+} binding and movement of the channel gate.

Methods

Channel expression and mutagenesis

The human Slo1 (hSlo1; KCNMA1; BK_{Ca}; U11058, hbr1; Tseng-Crank *et al.* 1994) channel alone, or hSlo1 and β1 (KCNMB1; 1 : 1 weight ratio) were transiently expressed in HEK-tsA cells using FuGENE 6 (Roche) as previously described (Avdonin *et al.* 2003). The mouse Slo1 β1 (mβ1; AF020711; Jiang *et al.* 1999) in pEGFP-N1 (BD Biosciences) was obtained from the laboratory of Dr R. Aldrich (Stanford University, Stanford, CA, USA). The mutant channels were constructed using PCR-based mutagenesis (Stratagene) and the sequences were verified.

Electrophysiology and data analysis

Macroscopic and single-channel ionic currents were recorded from excised inside-out patches at room temperature essentially as described previously (Tang *et al.* 2001; Santarelli *et al.* 2004). Patch electrodes (Warner) had

a typical initial resistance of 1.5–3 MΩ when filled with the solutions described below and the series resistance, ∼90% of the input resistance, was electronically compensated. Unless otherwise noted, macroscopic capacitative and leak currents were subtracted using a *P*/6 protocol as implemented in Pulse/PulseFit (HEKA). The current signal was filtered at 10 kHz through the built-in filter of the patch-clamp amplifier (AxoPatch 200A; Axon) and digitized at 100 kHz using an ITC-16 AD/DA interface (Instrutech).

Data were analysed using Pulse/PulseFit, PatchMachine (Tang *et al.* 2001; Avdonin *et al.* 2003), and IgorPro (WaveMetrics) running on Mac OS 9/10. Unless otherwise stated, instantaneous current amplitudes were estimated from single-exponential fits to the tail currents recorded at −50 mV following pulses to different voltages from the holding voltage of 0 mV. The voltage dependence of the instantaneous current size was then fitted with a simple Boltzmann function to estimate the normalized *G–V* curve characterized by the half-activation voltage ($V_{0.5}$) and the apparent equivalent charge movement (Q_{app}). The deactivation time courses were fitted by single exponentials excluding the initial 120 μs segment. A single-exponential fit to the voltage dependence of the time constant provided the value of the partial charge movement. To measure open probability and mean open duration, single-channel openings were idealized using the hidden Markov method as implemented in PatchMachine.

Statistical comparisons were made using the unpaired or paired *t* test, as appropriate. In some cases, ANOVA was followed by the Bonferroni *post hoc* test (DataDesk; Data Description). Statistical significance was assumed at $P \leq 0.05$. Where appropriate, data are presented as mean ± S.E.M. with all *n* values ≥ 3.

Reagents and solutions

Both the external and internal recording solutions contained (mM): 140 KCl, 11 EGTA and 10 Hepes; pH 7.2 adjusted with NMDG. The free Ca^{2+} concentration for these solutions was estimated at < 1 nM assuming 20 μM contaminating Ca^{2+} (Patcher's Power Tools v 1.0, F. Mendez; http://www.mpibpc.gwdg.de/abteilungen/140/software/) and also verified (Tang *et al.* 2001). In some experiments, the external solution contained (mM): 140 KCl, 2 $MgCl_2$ and 10 Hepes; pH 7.2 adjusted with NMDG to maintain high-resistance seals for longer durations. The 200 nM free Ca^{2+} internal solution contained (mM): 140 KCl, 0.6 $CaCl_2$, 10 HEDTA and 10 Hepes; pH 7.2 adjusted with NMDG. The 5 μM free Ca^{2+} internal solution contained (mM): 140 KCl, 6.1 $CaCl_2$, 10 HEDTA and 10 Hepes; pH 7.2 adjusted with NMDG. The 120 μM free Ca^{2+} internal solution contained (mM): 140 KCl, 0.12 $CaCl_2$ and 10 Hepes; pH 7.2 adjusted with NMDG. The 200 μM free Ca^{2+} internal solution contained (mM): 140 KCl, 0.2 $CaCl_2$ and 10 Hepes; pH 7.2 adjusted with NMDG.

Chloramine-T (Ch-T; Sigma-Aldrich) was dissolved in the internal solution immediately before use. Ch-T (2 mM) was manually applied with a pipette ensuring the addition of six times the bath volume (∼150 μl). With Ch-T present, channel current was monitored every 10 s for the characteristic features of oxidation by Ch-T: increased current amplitude and slowed deactivation. Once these characteristic changes reached steady-state levels (≤ 8 min), Ch-T was washed out with 1 ml of recording solution. Similar methods were used to apply 1 mM dithiothreitol (DTT; Amresco).

Simulation

Simulations of *G–V* curves based on the model of Horrigan and Aldrich (Horrigan & Aldrich, 2002) were performed using IgorPro essentially as described (Horrigan *et al.* 2005). The values of the Ca^{2+}-dependent parameters in the model were identical to those from Horrigan & Aldrich (2002) except for the following small changes that helped to better describe the experimental control data: allosteric factor D = 11, and allosteric factor C = 10.

Results

Methionine-to-leucine mutations in hSlo1

To determine whether the oxidation of one methionine residue within hSlo1 is responsible for the leftward shift of $V_{0.5}$ and the slowing of channel deactivation following oxidation by Ch-T, single methionine-to-leucine point mutants were constructed: 29 hSlo1 mutants in total (Fig. 1). Leucine was selected to replace methionine for the following reasons. The side chain of leucine is much less prone to oxidation but its other physical characteristics, such as size and hydrophobicity, are generally similar to those of the sulphur-containing methionine side chain. The non-polar nature of its side chain allows methionine to participate in forming hydrophobic contacts between different protein segments and substitution of methionine residues with leucine is expected to preserve such interactions. Consistent with this idea, methionine-to-leucine mutations are well tolerated and preserve near-wild-type-like properties in many proteins, including ion channels (Ciorba *et al.* 1997; Chen *et al.* 2000).

Ionic currents through the hSlo1 mutants transiently expressed in HEK cells were recorded in the inside-out patch-clamp configuration. In the absence of intracellular Ca^{2+}, the majority of the 29 single point mutants sufficiently expressed and behaved functionally similar to wild-type hSlo1, suggesting that the mutations did not cause a massive alteration in the channel structure.

Simple Boltzmann fits to the voltage dependence of the extrapolated instantaneous amplitudes of the tail currents elicited by prepulses to different voltages showed that the channels were half-activated at 150–200 mV with an apparent equivalent charge movement of ∼1 *e* (Table 1). The tail current kinetics of most of the mutants were indistinguishable from that of the wild-type channel with the time constants being ∼0.1 ms at −200 mV (Table 2). The activation kinetics of the mutants at depolarized voltages was also generally indistinguishable from that of the wild-type channel (data not shown).

A few notable exceptions, however, were observed with the mutations M285L, M314L and M536L. The M285L mutation in the pore region typically caused the channel to produce only very small currents and we could not detect any clear sign of tail current saturation even after increasing the prepulse depolarization to 360 mV. This observation is consistent with the possibility that the voltage dependence of activation of this mutant is shifted to extremely depolarized voltages. Since the standard *G–V* analysis was not possible for the M285L mutant, its oxidative sensitivity was determined by changes in the *I–V* or tail kinetics. The mutation M314L in the S6 segment produced a noticeable rightward shift of the overall voltage dependence of activation inferred from the normalized macroscopic *G–V* curve. The $V_{0.5}$ of the M314L mutant in the control condition prior to oxidant application was the only measurable $V_{0.5}$ value that differed significantly from that of wild-type hSlo1 (Table 1, $P \leq 0.0001$). Finally, the M536L mutation in the RCK1 domain significantly slowed the control deactivation kinetics (Table 2, $P \leq 0.0001$), but did not markedly alter the voltage dependence of activation.

No single methionine point mutation in hSlo1 completely eliminates the functional effects of oxidation

Treatment with the oxidant Ch-T (2 mM) increased the current amplitudes from each of the 29 single methionine point mutants in a voltage-dependent manner. As found with the wild-type channel (Fig. 2*A*, left), the current increase was accompanied by a significant leftward shift of the *G–V* curve from every mutant for which the analysis was possible (Fig. 2*B*, Supplementary Fig. 1*A*). The M314L mutant, though exhibiting the large right-shifted control $V_{0.5}$ value, also responded to Ch-T treatment by shifting the $V_{0.5}$ value to the more negative direction. The mean shift of $V_{0.5}$ caused by Ch-T application ($\Delta V_{0.5}$) in each mutant was typically −30 to −40 mV and we found no statistically significant difference in $\Delta V_{0.5}$ among the wild-type and mutant channels (Fig. 2*B*; Table 1, $P \geq 0.98$). Besides the leftward shift in $V_{0.5}$, treatment of hSlo1 with Ch-T produced a slight decrease in the apparent

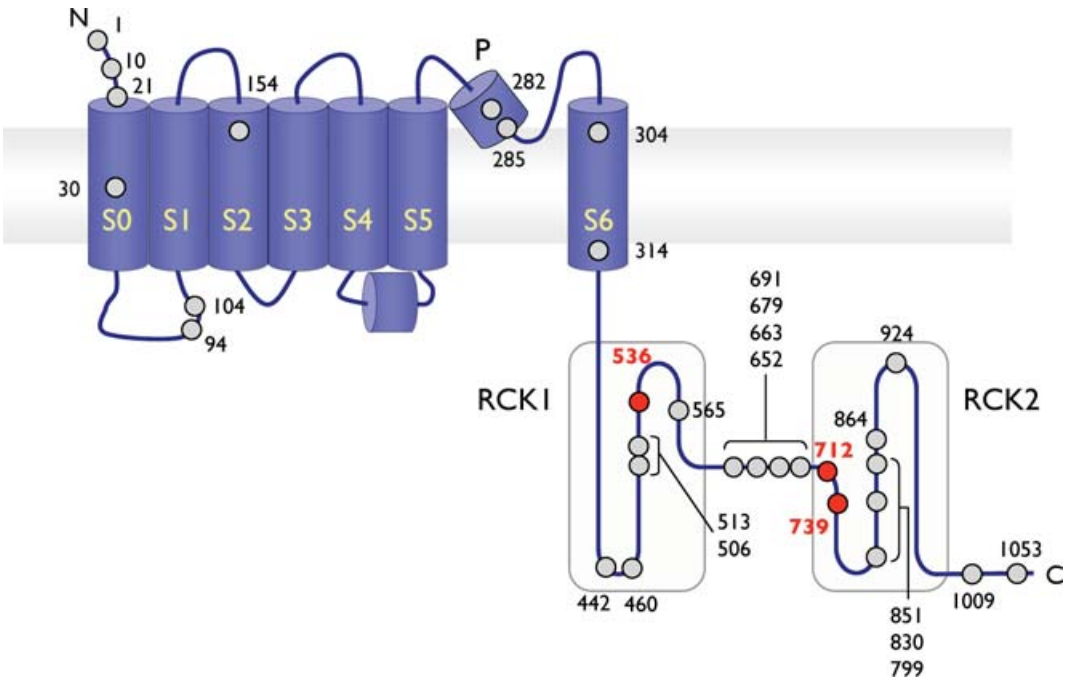

Figure 1. Schematic representation of the methionine residues within hSlo1
A linear depiction of a single hSlo1 subunit illustrating the seven putative transmembrane-spanning segments (S0–S6), the pore region (P), and the 30 methionine residues (circles). Critical met residues are shown in bold and red. The two shaded, large intracellular areas represent RCK1 and RCK2 domains. The S4–S5 linker is included as suggested by the results of Long *et al.* (2005). Not drawn to scale.

Table 1. Steady-state activation properties of the wild-type and single point mutant channels in the virtual absence of Ca^{2+}. (N.D. not determined)

Channel	Pre-$V_{0.5}$ (mV)	Post-$V_{0.5}$ (mV)	$\Delta V_{0.5}$ (mV)	Pre-Q_{app} (*e*)	Post-Q_{app} (*e*)	ΔQ_{app} (*e*)
WT	171.9 ± 4.5	140.6 ± 6.1	−31.3 ± 3.3	1.09 ± 0.16	0.84 ± 0.09	−0.25 ± 0.07
M10L	168.6 ± 10	130.3 ± 16	−38.3 ± 9.6	1.26 ± 0.14	0.96 ± 0.01	−0.29 ± 0.09
M21L	169.6 ± 12	134.0 ± 8.6	−35.6 ± 7.8	1.16 ± 0.10	0.80 ± 0.07	−0.35 ± 0.07
M30L	176.0 ± 2.9	126.5 ± 9.0	−49.5 ± 9.9	1.11 ± 0.25	0.85 ± 0.06	−0.27 ± 0.09
M94L	181.3 ± 11	156.2 ± 9.8	−25.1 ± 2.9	1.07 ± 0.04	0.84 ± 0.06	−0.22 ± 0.06
M104L	146.2 ± 6.5	101.9 ± 9.3	−44.2 ± 3.2	1.16 ± 0.11	0.86 ± 0.12	−0.30 ± 0.03
M154L	163.3 ± 18	126.7 ± 15	−36.5 ± 4.3	1.09 ± 0.25	0.76 ± 0.06	−0.33 ± 0.07
M282L	189.7 ± 3.9	143.0 ± 7.6	−46.6 ± 5.2	1.00 ± 0.04	0.86 ± 0.05	−0.14 ± 0.07
M285L	N.D.	N.D.	N.D.	N.D.	N.D.	N.D.
M304L	187.5 ± 3.0	144.3 ± 6.9	−43.2 ± 4.3	0.95 ± 0.07	0.80 ± 0.07	−0.15 ± 0.03
M314L	222.4 ± 2.8	179.3 ± 4.3	−43.1 ± 5.0	0.91 ± 0.78	0.78 ± 0.03	−0.13 ± 0.04
M442L	202.4 ± 4.8	173.4 ± 7.5	−29.0 ± 5.4	1.02 ± 0.03	0.90 ± 0.03	−0.13 ± 0.05
M460L	175.5 ± 6.8	134.1 ± 3.1	−41.4 ± 4.3	1.12 ± 0.07	0.96 ± 0.08	−0.16 ± 0.08
M506L	157.5 ± 6.8	119.1 ± 7.0	−38.4 ± 6.8	1.15 ± 0.03	0.94 ± 0.10	−0.21 ± 0.03
M513L	165.8 ± 9.0	134.7 ± 11	−31.2 ± 4.4	0.87 ± 0.05	0.74 ± 0.06	−0.13 ± 0.01
M536L	167.3 ± 4.8	138.3 ± 9.5	−29.0 ± 5.5	0.91 ± 0.09	0.77 ± 0.06	−0.14 ± 0.05
M565L	174.7 ± 7.1	128.6 ± 5.5	−46.0 ± 3.2	1.03 ± 0.11	0.77 ± 0.08	−0.26 ± 0.07
M652L	174.1 ± 4.0	137.9 ± 8.6	−36.2 ± 6.3	1.01 ± 0.07	0.76 ± 0.09	−0.25 ± 0.02
M663L	163.5 ± 4.5	128.5 ± 7.0	−36.9 ± 6.8	1.00 ± 0.03	0.76 ± 0.03	−0.24 ± 0.002
M679L	153.5 ± 7.4	126.4 ± 5.0	−27.1 ± 7.5	1.27 ± 0.19	0.84 ± 0.04	−0.42 ± 0.03
M691L	174.0 ± 2.9	143.3 ± 5.5	−31.6 ± 5.5	1.15 ± 0.04	1.08 ± 0.04	−0.07 ± 0.01
M712L	170.4 ± 8.5	126.4 ± 15	−44.0 ± 8.7	1.07 ± 0.13	0.95 ± 0.05	−0.12 ± 0.05
M739L	161.1 ± 5.6	137.7 ± 9.6	−23.4 ± 5.5	1.01 ± 0.09	0.80 ± 0.05	−0.21 ± 0.06
M799L	143.0 ± 3.7	114.7 ± 1.6	−28.3 ± 2.3	1.25 ± 0.13	1.12 ± 0.10	−0.12 ± 0.04
M830L	159.2 ± 13	128.5 ± 15	−30.7 ± 2.4	0.97 ± 0.09	0.75 ± 0.09	−0.22 ± 0.03
M851L	178.2 ± 7.1	139.1 ± 7.7	−39.1 ± 1.9	1.01 ± 0.13	0.81 ± 0.09	−0.20 ± 0.06
M864L	157.5 ± 6.4	116.0 ± 7.8	−41.5 ± 8.9	0.85 ± 0.10	0.69 ± 0.11	−0.16 ± 0.07
M924L	154.0 ± 12	120.8 ± 11	−33.2 ± 3.9	1.38 ± 0.18	0.94 ± 0.03	−0.43 ± 0.04
M1009L	160.3 ± 6.4	112.2 ± 9.1	−48.1 ± 3.1	0.97 ± 0.13	0.80 +0.08	−0.17 ± 0.05
M1053L	167.1 ± 4.0	138.6 ± 1.1	−28.5 ± 3.7	1.09 ± 0.08	0.84 ± 0.06	−0.25 ± 0.03

charge movement (Q_{app}) determined from the normalized *G–V* curve (Fig. 2*A*, left). A similar decrease in Q_{app} due to modification by Ch-T (ΔQ_{app}) was retained in every mutant analysed (Fig. 2*C*; Table 1) and no statistically significant difference in the magnitude of ΔQ_{app} among the channels was observed ($P \geq 0.99$).

In addition to maintaining the changes in steady-state activation primarily reflected in $\Delta V_{0.5}$, the single methionine point mutants also exhibited the characteristic slowing of channel deactivation that was displayed by the wild-type channel following treatment with Ch-T (Fig. 2*A*, centre; Supplementary Fig. 1*B*). The oxidative modification led to a significant increase in the values of the time constants of deactivation at each voltage tested, including the most hyperpolarized potential (−200 mV; Fig. 2*A*, right; Supplementary Fig. 1*C*; Table 2), at which even the M536L mutant, whose deactivation kinetics before Ch-T treatment was slower than that of the wild-type channel, exhibited clear slowing of deactivation kinetics similar to that of wild-type hSlo1 ($P = 0.77$). The fractional increases in the deactivation time constants ($\tau_{Ch\text{-}T}/\tau_{Ctl}$) of the wild-type and point mutant channels were statistically indistinguishable (Fig. 2*D*, Table 2, $P \geq 0.99$).

Therefore, each individual methionine point mutant of hSlo1 retained the hallmark increase in open probability and the slowing of deactivation caused by treatment with Ch-T. This observation indicated that no single methionine residue within the channel was solely responsible for the functional effects of the oxidation.

Contemporaneous mutation of M536, M712 and M739 removes the oxidative sensitivity

None of the individual methionine-to-leucine mutations eliminated the Ch-T sensitivity in a statistically significant manner. Furthermore, the mean $\Delta V_{0.5}$ and $\tau_{Ch\text{-}T}/\tau_{Ctl}$ values from different mutant channels were statistically indistinguishable. However, we did notice some statistically non-significant trends with regard to two methionine residues located within the RCK1 and RCK2 domains; the degree of tail slowing of the M536L

Table 2. Deactivation kinetics of the wild-type and single point mutant channels in the virtual absence of Ca^{2+}. (N.D. not determined)

Channel	Pre-τ (−200 mV) (ms)	Post-τ (−200 mV) (ms)	$\Delta\tau$ (ms)	Ratio (Post-τ/Pre-τ)
WT	0.093 ± 0.004	0.144 ± 0.008	0.051 ± 0.007	1.55
M10L	0.085 ± 0.003	0.117 ± 0.006	0.032 ± 0.003	1.38
M21L	0.088 ± 0.005	0.123 ± 0.016	0.035 ± 0.017	1.40
M30L	0.104 ± 0.007	0.142 ± 0.022	0.039 ± 0.016	1.37
M94L	0.079 ± 0.003	0.098 ± 0.009	0.019 ± 0.009	1.25
M104L	0.096 ± 0.012	0.139 ± 0.039	0.043 ± 0.028	1.44
M154L	0.095 ± 0.007	0.147 ± 0.001	0.052 ± 0.007	1.55
M282L	0.081 ± 0.003	0.127 ± 0.007	0.046 ± 0.005	1.57
M285L	N.D.	N.D.	N.D.	N.D.
M304L	0.095 ± 0.003	0.125 ± 0.007	0.030 ± 0.006	1.31
M314L	0.072 ± 0.002	0.088 ± 0.005	0.016 ± 0.004	1.22
M442L	0.082 ± 0.006	0.102 ± 0.011	0.021 ± 0.005	1.25
M460L	0.092 ± 0.009	0.123 ± 0.011	0.031 ± 0.002	1.34
M506L	0.099 ± 0.014	0.126 ± 0.002	0.027 ± 0.012	1.27
M513L	0.085 ± 0.003	0.122 ± 0.004	0.038 ± 0.007	1.44
M536L	0.167 ± 0.011	0.206 ± 0.022	0.038 ± 0.014	1.20
M565L	0.086 ± 0.010	0.133 ± 0.014	0.048 ± 0.018	1.56
M652L	0.086 ± 0.010	0.137 ± 0.023	0.051 ± 0.017	1.59
M663L	0.098 ± 0.003	0.158 ± 0.013	0.060 ± 0.010	1.61
M679L	0.079 ± 0.003	0.114 ± 0.008	0.035 ± 0.004	1.43
M691L	0.089 ± 0.006	0.127 ± 0.012	0.038 ± 0.007	1.43
M712L	0.090 ± 0.005	0.135 ± 0.024	0.045 ± 0.020	1.50
M739L	0.089 ± 0.005	0.114 ± 0.009	0.025 ± 0.005	1.29
M799L	0.090 ± 0.005	0.126 ± 0.011	0.036 ± 0.010	1.40
M830L	0.093 ± 0.009	0.135 ± 0.022	0.042 ± 0.014	1.46
M851L	0.082 ± 0.005	0.125 ± 0.017	0.043 ± 0.014	1.53
M864L	0.093 ± 0.007	0.172 ± 0.028	0.072 ± 0.027	1.85
M924L	0.103 ± 0.003	0.125 ± 0.004	0.014 ± 0.009	1.21
M1009L	0.100 ± 0.009	0.147 ± 0.016	0.047 ± 0.009	1.47
M1053L	0.087 ± 0.009	0.114 ± 0.009	0.027 ± 0.016	1.31

mutant and the mean $\Delta V_{0.5}$ of the M739L mutant appeared smaller than those for the wild-type channel. Nevertheless, a channel containing both the M536L and M739L mutations retained Ch-T sensitivity statistically similar to that of wild-type hSlo1 (Fig. 4*A*; $P = 0.99$). To test whether the additional mutation of a third methionine residue located within close proximity to M739 based on the linear sequence was necessary to prevent the shift in $V_{0.5}$ following treatment with Ch-T, a triple mutant with the mutations M536L, M712L and M739L spanning the RCK domains was created.

The steady-state activation and kinetic properties of the M536L–M712L–M739L mutant, referred to as Triple Met hereafter, were similar to those of the wild-type channel prior to oxidant treatment (Fig. 3). However, in striking contrast with the large increase in current amplitude exhibited by wild-type hSlo1 following application of Ch-T, Triple Met demonstrated no change in current amplitude after the modification as shown in Fig. 3*A*. The currents recorded from the Triple Met channel at other voltages were also unaltered by Ch-T (Fig. 3*B*). Furthermore, Triple Met displayed no significant leftward shift of $V_{0.5}$ following the oxidant treatment (Fig. 3*C*). The insensitivity of the mutant $V_{0.5}$ to Ch-T pooled from multiple experiments is further illustrated in Fig. 3*D*. Whereas the wild-type channels exhibited a mean $\Delta V_{0.5}$ value of −30 mV, the Triple Met mean $\Delta V_{0.5}$ value was -2.4 ± 1.3 mV ($n = 8$); modification by Ch-T failed to cause a statistically significant difference in $V_{0.5}$ of the mutant channel (Fig. 3*D*, left; Table 3, $P = 0.1$). Unlike the decrease in the steepness of the *G*–*V* slope exhibited by wild-type hSlo1 following application of Ch-T, oxidation did not significantly alter the Triple Met mean Q_{app} value (Fig. 3*D*, right; $\Delta Q_{app} = -0.17 \pm 0.09$; $P > 0.1$). Even when the duration of the treatment with Ch-T (2 mM) was increased to 15 min, nearly twice as long than usual, no change in the peak current amplitude or deactivation kinetics was observed (data not shown).

Slowing of channel deactivation at extreme negative voltages where the closing rate constants dominate and the channel activation is negligible is another characteristic feature of Ch-T modification of wild-type hSlo1. Triple

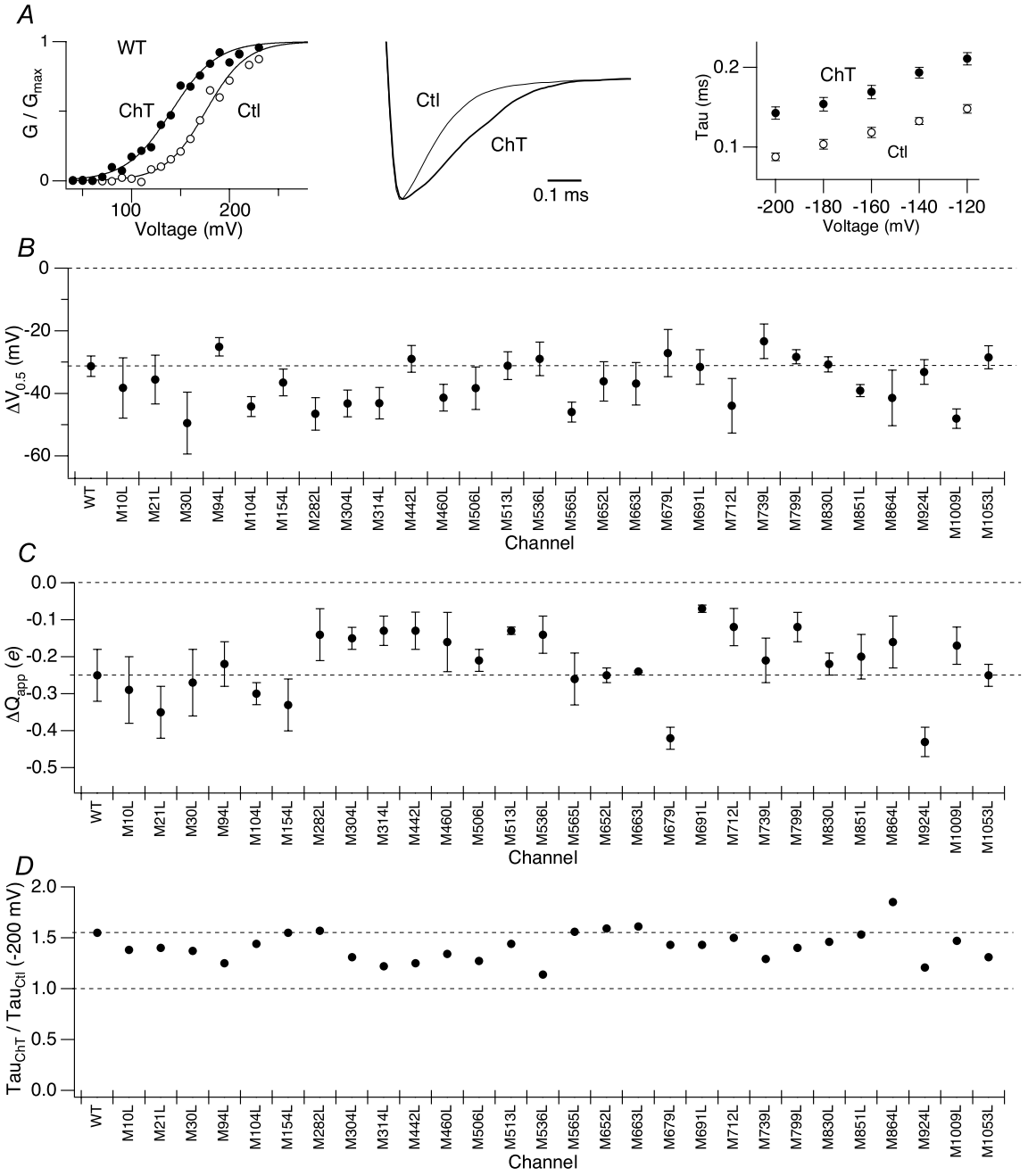

Figure 2. Individual mutation of single methionine residues within hSlo1 does not remove the functional sensitivity to oxidation by Ch-T

A, left: representative wild-type hSlo1 *G–V* curve before (○) and after (●) modification by 2 mM Ch-T. The macroscopic currents were elicited by pulses to different test voltages from the holding voltage of 0 mV. Centre: scaled tail currents recorded at −200 mV after pulses to 180 mV before (thin sweep) and after (thick sweep) Ch-T modification. Right: voltage dependence of the deactivation time constants for wild-type hSlo1 before (○) and after (●) application of Ch-T. *B*, mean $\Delta V_{0.5}$ and *C*, ΔQ_{app} caused by treatment with Ch-T from the single point-mutant channels compared with those of wild-type hSlo1. See Table 1 for mean ± S.E.M. values. See Supplementary Fig. 1*A* for single point-mutant *G–V* curves and results regarding the M285L mutant. *D*, relative increase in the time constant due to treatment with Ch-T measured at −200 mV for the single point-mutant channels compared with that of wild-type hSlo1. See Table 2 for mean ± S.E.M. values; $n = 3$. See Supplementary Fig. 1*B* for single point-mutant scaled tail currents and Supplementary Fig. 1*C* for the voltage dependence of the deactivation time constants of the single point-mutant channels.

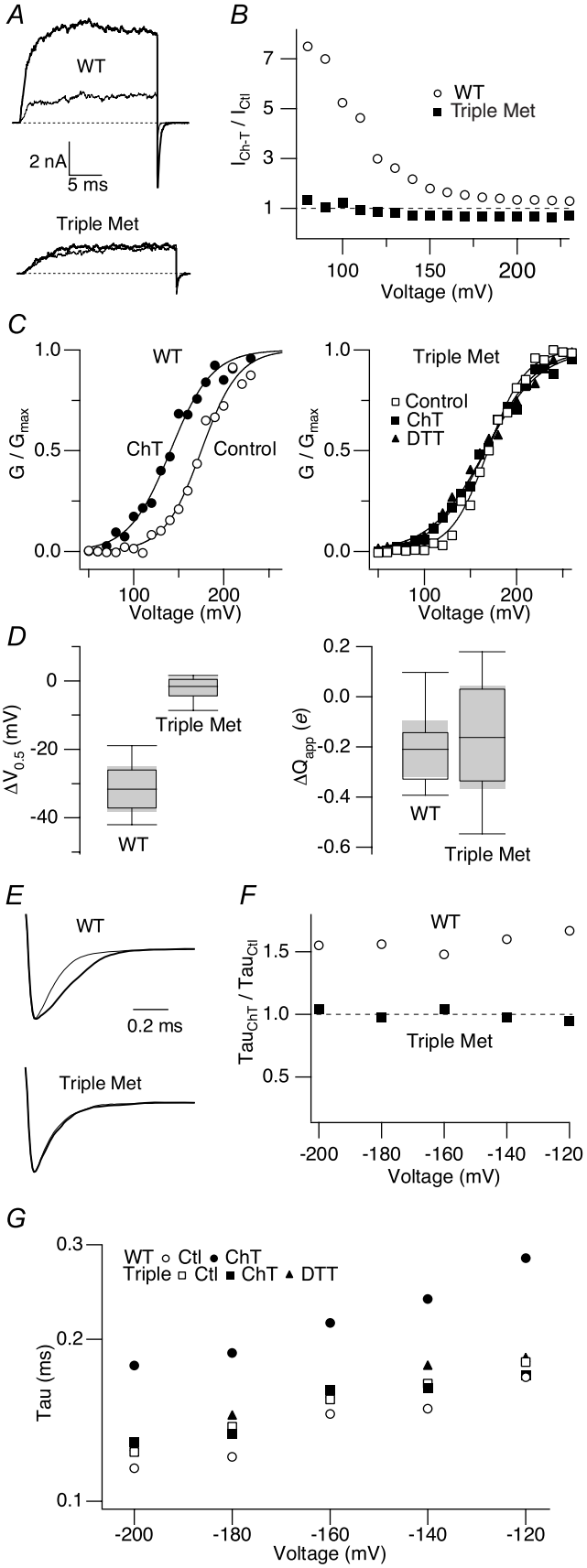

Met demonstrated no significant slowing of deactivation at any of the voltages examined (Fig. 3*E–G*, Table 4). In addition, the voltage dependence of the tail time constant for both wild-type hSlo1 and the Triple Met mutant did not change following treatment with Ch-T (Fig. 3*G*).

While Ch-T preferentially oxidizes methionine residues in many proteins, it could also induce cysteine oxidation (Vogt, 1995). Previous results using a systematic removal of cysteine residues demonstrated that cysteine oxidation does not underlie the functional changes caused by Ch-T in wild-type hSlo1 (Tang *et al.* 2001). This is further corroborated by the observation here that the Ch-T sensitivity is not discernable in Triple Met, which contains only methionine mutations. However, any underlying sensitivity of the Triple Met mutant might have been masked or counteracted by the effect of cysteine oxidation, which generally decreases the open probability of Slo1 (Dichiara & Reinhart, 1997; Soto *et al.* 2002; Tang *et al.* 2004). To rule against this possibility, DTT, a reducing agent capable of reducing oxidized cysteine, was applied to the Triple Met channel following oxidation with Ch-T (Fig. 3*C*). The mean $V_{0.5}$ value after DTT treatment (159.6 ± 5.9 mV, $n = 3$) was not significantly different from those values before or after Ch-T modification (161.1 ± 4.8 and 158.7 ± 4.3 mV, respectively; $P = 0.9$). The reducing agent DTT also failed to alter the Triple Met deactivation kinetics (Fig. 3*G*; $P = 0.5$). The lack of any DTT effect generally favours the idea that cysteine oxidation played no major role. Taken together with the finding here that the Ch-T sensitivity is not observed in Triple Met, Ch-T appears to be indeed a

Figure 3. Concurrent mutation of M536, M712 and M739 in hSlo1 eliminates the functional effects of methionine oxidation
A, representative wild-type hSlo1 (top) and Triple Met mutant (bottom) currents before (thin sweep) and after (thick sweep) Ch-T treatment. The currents were elicited in response to pulses from 0 to 120 mV, a voltage at which the channel open probability is not saturated. Dotted lines represent the zero current level. *B*, relative changes in current amplitude caused by Ch-T as a function of voltage for wild-type hSlo1 (○) and Triple Met (■). *C*, wild-type hSlo1 (circles, left) and Triple Met (squares, right) *G–V* curves before (open symbols) and after (filled symbols) modification by Ch-T and DTT (triangles). See Table 3 for mean ± S.E.M. values; $n = 8$. *D*, box-plots summarizing the changes in $V_{0.5}$ (left) and Q_{app} (right) induced by Ch-T in wild-type hSlo1 and the Triple Met mutant. The shaded region represents the 95% confidence interval of the median. A negative Q_{app} value denotes a decrease in the steepness of the *G–V* curve. *E*, wild-type hSlo1 (top) and Triple Met (bottom) scaled tail currents recorded at −200 mV after pulses to 180 mV before (thin sweep) and after (thick sweep) Ch-T application. *F*, relative changes in the value of the wild-type hSlo1 (○) and Triple Met (■) deactivation time constants due to treatment with Ch-T as a function of voltage. *G*, voltage dependence of the deactivation time constant for wild-type hSlo1 (circles) and the Triple Met mutant (squares) before (open symbols) and after (filled symbols) modification by Ch-T and DTT (triangles). See Table 4 for mean ± S.E.M. values; $n = 8$.

Table 3. Steady-state activation properties of the wild-type, multiple M-to-L, and M-to-E mutant channels in the virtual absence of Ca^{2+}

Channel	Pre-$V_{0.5}$ (mV)	Post-$V_{0.5}$ (mV)	$\Delta V_{0.5}$ (mV)	Pre-Q_{app} (*e*)	Post-Q_{app} (*e*)	ΔQ_{app} (*e*)
WT	171.9 ± 4.5	140.6 ± 6.1	−31.3 ± 3.3	1.1 ± 0.16	0.84 ± 0.09	−0.25 ± 0.07
Triple Met	161.1 ± 4.8	158.7 ± 4.3	−2.4 ± 1.3	1.1 ± 0.07	0.90 ± 0.06	−0.17 ± 0.09
M536L–M712L	177.9 ± 5.6	144.0 ± 8.8	−33.9 ± 3.3	0.7 ± 0.05	0.61 ± 0.02	−0.07 ± 0.07
M536L–M739L	166.5 ± 6.6	141.8 ± 5.4	−24.8 ± 2.7	1.1 ± 0.01	0.97 ± 0.01	−0.11 ± 0.003
M712L–M739L	171.5 ± 6.0	131.8 ± 4.4	−39.8 ± 7.9	1.0 ± 0.15	0.90 ± 0.09	−0.15 ± 0.10
M460L–M712L–M739L	164.0 ± 2.8	125.3 ± 3.1	−38.6 ± 2.5	1.2 ± 0.10	0.97 ± 0.12	−0.28 ± 0.17
M652L–M712L–M739L	123.8 ± 4.9	90.18 ± 3.3	−33.6 ± 6.9	1.3 ± 0.04	1.03 ± 0.05	−0.28 ± 0.005
M712L–M739L–M851L	152.7 ± 3.4	121.6 ± 4.4	−31.1 ± 1.1	1.2 ± 0.11	1.01 ± 0.11	−0.22 ± 0.029
M563E	226.7 ± 4.4	194.1 ± 7.8	−32.7 ± 5.3	0.9 ± 0.02	0.77 ± 0.08	−0.16 ± 0.059
M712E	140.7 ± 4.0	128.2 ± 5.0	−12.5 ± 2.8	1.2 ± 0.11	0.91 ± 0.09	−0.27 ± 0.058
M739E	109.6 ± 2.6	99.73 ± 3.1	−9.8 ± 2.3	1.3 ± 0.03	0.95 ± 0.06	−0.35 ± 0.04

Table 4. Deactivation kinetics of the wild-type, multiple M-to-L, and M-to-E mutant channels in the virtual absence of Ca^{2+}

Channel	Pre-τ (−200 mV) (ms)	Post-τ (−200 mV) (ms)	Delta τ (ms)	Ratio (Post-τ/Pre-τ)
WT	0.093 ± 0.004	0.144 ± 0.008	0.051 ± 0.007	1.55
Triple Met	0.144 ± 0.012	0.129 ± 0.009	−0.015 ± 0.011	0.90
M536L–M712L	0.164 ± 0.011	0.243 ± 0.016	0.079 ± 0.010	1.48
M536L–M739L	0.115 ± 0.009	0.141 ± 0.012	0.018 ± 0.022	1.23
M712L–M739L	0.100 ± 0.011	0.131 ± 0.011	0.031 ± 0.019	1.31
M460L–M712L–M739L	0.105 ± 0.016	0.156 ± 0.022	0.042 ± 0.001	1.49
M652L–M712L–M739L	0.121 ± 0.005	0.163 ± 0.017	0.042 ± 0.016	1.35
M712L–M739L–M851L	0.097 ± 0.002	0.121 ± 0.002	0.024 ± 0.002	1.25
M563E	0.086 ± 0.005	0.110 ± 0.005	0.025 ± 0.004	1.27
M712E	0.098 ± 0.001	0.111 ± 0.008	0.013 ± 0.008	1.14
M739E	0.120 ± 0.004	0.139 ± 0.004	0.019 ± 0.003	1.16

methionine-specific modifying reagent with regard to the functional effects of hSlo1 oxidation.

Double mutations involving M536, M712 and M739 fail to eliminate the oxidative sensitivity

Individual methionine-to-leucine mutations did not remove the sensitivity of the channels to treatment with Ch-T, but the triple mutation M536L–M712L–M739L effectively abolished the functional effects due to modification by the oxidant. Thus, we examined whether double mutations encompassing combinations of these key methionine residues retained any Ch-T sensitivity. All channels containing mutations at only two of the three key methionine sites (M536L–M712L, M536L–M739L and M712L–M739L) maintained the leftward shift of the *G–V* curve and the slowing of deactivation kinetics after treatment with Ch-T in a manner statistically indistinguishable from that of wild-type hSlo1 (Fig. 4*A*, Tables 3 and 4, $P \geq 0.9$). In addition, the modification time courses of the single- and double-mutant channels did not appreciably differ from that of wild-type hSlo1 (data not shown). Therefore, the requirement of the triple mutation to abolish the functional effects of modification by Ch-T suggests that the oxidation of one of these three residues must be sufficient to confer the observed oxidative sensitivity.

Other triple mutations do not remove the oxidative sensitivity

The results presented above did not exclude the possibility that other triple methionine-to-leucine mutations within hSlo1 could also disrupt the oxidative sensitivity. A systematic examination of all other triple mutants covering the 29 methionine residues (i.e. 3653 combinations) to completely exclude this possibility was clearly impractical. Thus, we used a more focused and selected approach to ensure the specificity/uniqueness of the triple mutation M536L–M712L–M739L. Other methionine residues located near the identified critical locations (M460, M652, M851) were selected and triple mutants involving these nearby residues (M460L–M712L–M739L, M652L–M712L–M739L and M712L–M739L–M851L)

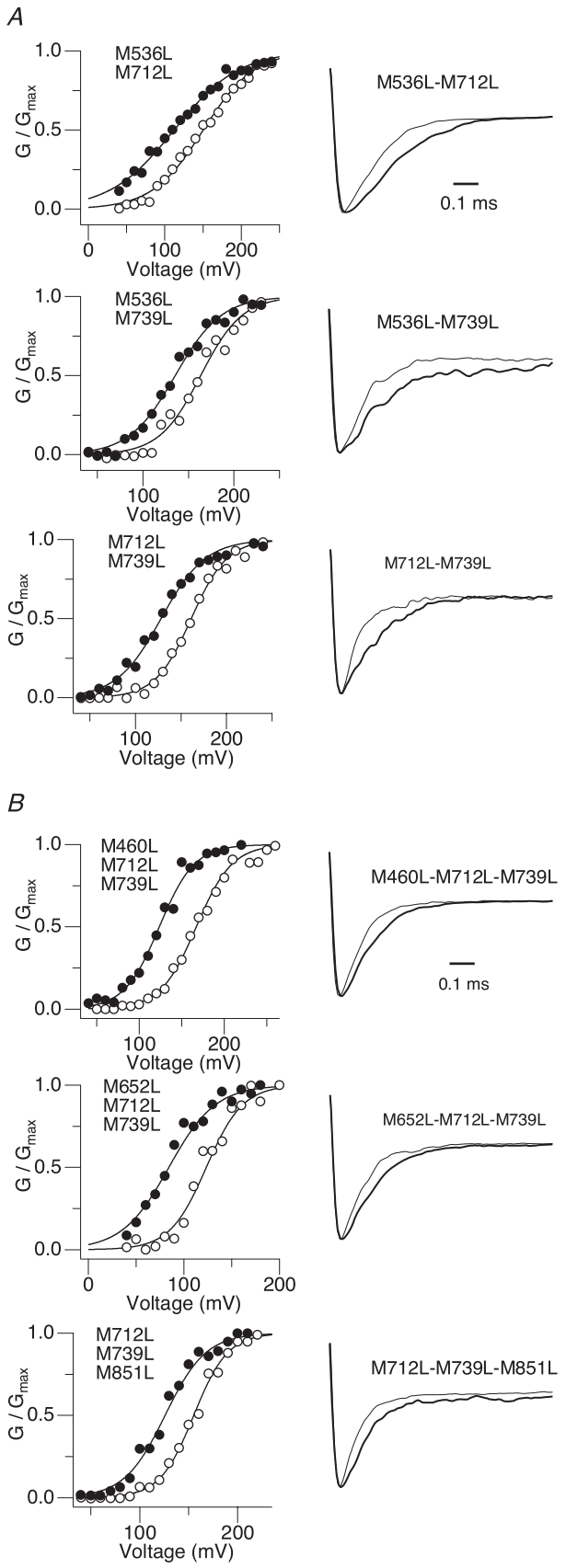

were examined for Ch-T sensitivity. Each of these *other* triple mutants also exhibited a robust increase in the channel open probability and slowing of deactivation kinetics that were statistically indistinguishable from those of the wild-type channel (Fig. 4*B*, Tables 3 and 4, $P \geq 0.9$). Therefore, even a seemingly small variation in the triple mutation sequence reinstates the channel's sensitivity to oxidation, affirming the specificity of the sequence set M536–M712–M739.

The presence of β1 does not restore wild-type-like Ch-T sensitivity to the Triple Met mutant channel

Whereas the triple mutation M536L–M712L–M739L abolishes the functional outcomes of methionine oxidation within hSlo1, the typical effects caused by Ch-T treatment of the wild-type channel are noticeably enhanced by the presence of the auxiliary β1 subunit; the mean $\Delta V_{0.5}$ is about twice as large (-75 mV) and the slowing of the channel deactivation is much more dramatic (Santarelli *et al.* 2004). Since the introduction of β1 reinstates Ca^{2+} sensitivity to an otherwise Ca^{2+}-insensitive mutant Slo1 channel (Qian & Magleby, 2003), we asked whether coexpression with β1 could restore this remarkably large oxidation-induced shift of $V_{0.5}$ and slowing of the deactivation kinetics in the Triple Met channel, which is essentially Ch-T insensitive when expressed alone.

The slower activation and deactivation exhibited by Triple Met + β1 confirmed the functional presence of the auxiliary subunit in the channel complex (Fig. 5*A*). However, the Triple Met + β1 channel complex did not display the striking enhancement of the functional effects of Ch-T treatment typically observed with the wild-type hSlo1 + β1 complex. The mean $\Delta V_{0.5}$ value for Triple Met + β1 (-22 ± 3.4 mV, $n = 5$) was 70% less than that of WT + β1 (-75 ± 3.5 mV; Fig. 5*B*), with certain experiments producing $\Delta V_{0.5}$ values closer to -10 mV for Triple Met + β1. In addition, the channel complex consisting of the Triple Met α subunit and

Figure 4. As compared with M536L–M712L–M739L, other combinations of methionine mutations do not remove Ch-T sensitivity
A, left: double methionine mutant *G–V* curves before (open symbols) and after (filled symbols) treatment with Ch-T. See Table 3 for mean ± S.E.M. values; $n = 3$. Right: scaled tail currents recorded at -200 mV after pulses to 180 mV before (thin sweep) and after (thick sweep) Ch-T application. See Table 4 for mean ± S.E.M. values. *B*, left: alternative combinations of triple methionine mutant *G–V* curves before (open symbols) and after (filled symbols) treatment with Ch-T. See Table 3 for mean ± S.E.M. values; $n = 3$. Right: scaled tail currents recorded at -200 mV after pulses to 180 mV before (thin sweep) and after (thick sweep) Ch-T application. See Table 4 for mean ± S.E.M. values.

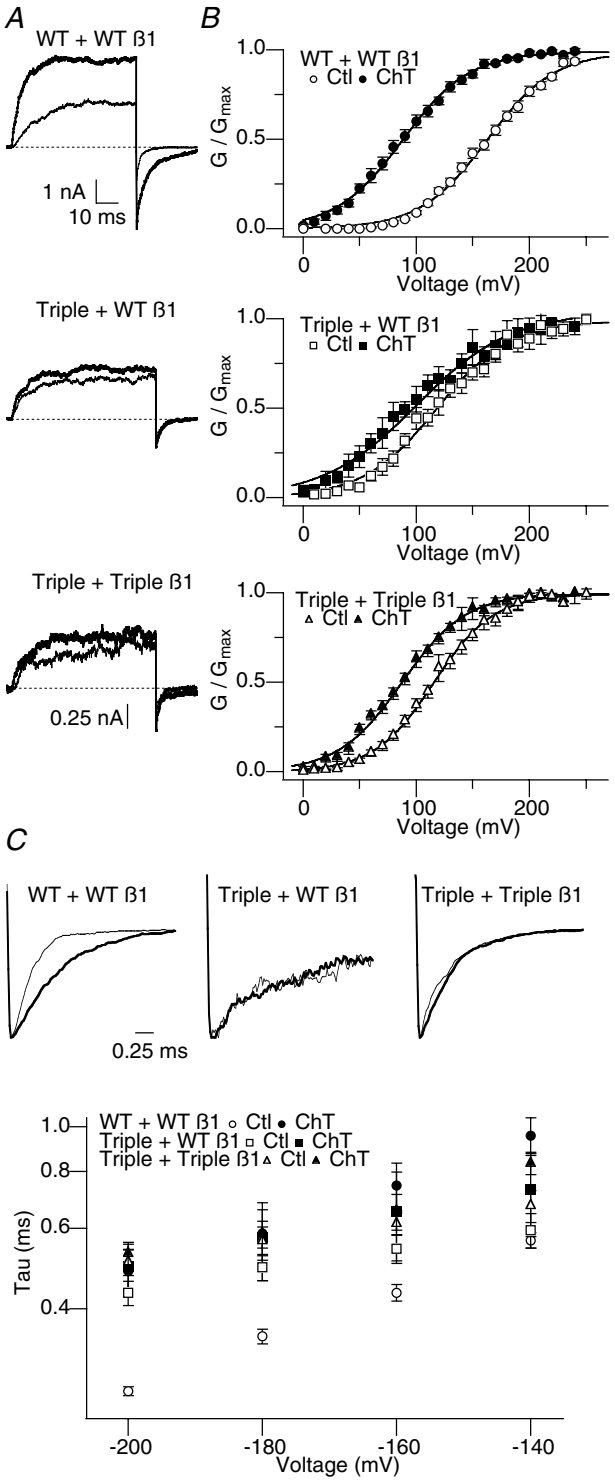

Figure 5. Coexpression of β1 with the Triple Met mutant does not restore wild-type hSlo1 + β1-like Ch-T sensitivity
A, representative wild-type hSlo1 + β1 (top), Triple Met mutant + β1 (middle), and Triple Met mutant + Triple mutant β1 currents (bottom) before (thin sweep) and after (thick sweep) Ch-T treatment. The activation currents were elicited in response to pulses from 0 to 110 mV and the dotted lines represent the zero current level. The Triple mutant β1 contains methionine-to-leucine mutations at M7, located at the intracellular amino terminus, and M23 and M177, located within the transmembrane-spanning segments. *B*, *G–V* curves before and after modification by Ch-T. The wild-type hSlo1 + β1 (top) mean $V_{0.5}$ values for the results obtained before (○) and after (●) Ch-T application were 163.8 ± 3.8 and 89.2 ± 4.1 mV ($\Delta V_{0.5}$ range −50 to −99 mV), respectively. The Triple Met mutant + β1 (middle) mean $V_{0.5}$ values for the results obtained before (□) and after (■) Ch-T application were 119.7 ± 7.4 and 96.8 ± 9.9 mV ($\Delta V_{0.5}$ range −10 to −33 mV), respectively. The Triple Met mutant + Triple mutant β1 (bottom) mean $V_{0.5}$ values for the results obtained before (△) and after (▲) Ch-T application were 116.8 ± 4.9 and 88.5 ± 4.5 mV ($\Delta V_{0.5}$ range −23 to −33 mV), respectively; ($n = 5$). *C*, top: representative wild-type hSlo1 + β1 (left), Triple Met mutant + β1 (middle), and Triple Met mutant + Triple mutant β1 (right) scaled tail currents recorded at −200 mV after pulses to 180 mV before (thin sweep) and after (thick sweep) Ch-T treatment. Bottom: voltage dependence of the deactivation time constant for wild-type hSlo1 + β1 (circles), Triple Met mutant + β1 (squares), and Triple Met mutant + Triple mutant β1 (triangles) before (open symbols) and after (filled symbols) Ch-T treatment.

a mutant β1 (Triple β1), in which three methionine residues (M7, M23 and M177) have been concurrently mutated to leucine essentially rendering it Ch-T insensitive (Santarelli *et al.* 2004), exhibited Ch-T sensitivity similar to that of Triple Met + wild-type β1 ($P = 0.12$), thereby excluding any possible effects from oxidation within β1. Furthermore, Triple Met plus either the wild-type or Triple β1 exhibited no significant slowing of channel deactivation following treatment with Ch-T (Fig. 5*C*; $P = 0.4$ and 0.8, respectively). Therefore, the presence of β1 is not capable of returning wild-type hSlo1 + β1-like Ch-T sensitivity to the Ch-T-insensitive Triple Met channel, suggesting the critical role of the amino acids M536, M712 and M739 in mediating the oxidant sensitivity.

Hydrophilic substitution at M712 or M739 mimics the oxidized channel

Changes in protein function caused by methionine oxidation have been attributed to the drastic change in the physical characteristic of the side chain from flexible and hydrophobic in nature for methionine to stiff and polar/hydrophilic for methionine sulfoxide (met-O). Such changes disrupt the non-polar milieu normally provided by methionine. For example, oxidation of a methionine residue in the distal N-terminal segment of the ball domain in a *Shaker* potassium channel mimics the introduction of a charged amino acid into the otherwise non-polar area and drastically slows the inactivation time course (Ciorba *et al.* 1997). Thus, we hypothesized that oxidation of any one of the three identified critical methionine residues shifts the $V_{0.5}$ and slows the deactivation in part by inserting a polar element into a normally hydrophobic local environment. In its simplest form, this idea predicts that introduction of a charged amino acid at any of the three key sites should mimic the effects of Ch-T, such that the control $V_{0.5}$ value should be left-shifted and

the deactivation kinetics should be slower, and that these parameters should be insensitive to Ch-T treatment.

The prediction was tested with the hSlo1 mutants M536E, M712E and M739E, in which a negatively charged glutamate was introduced at the respective methionine position. Consistent with the supposition, the control $V_{0.5}$ values for the M712E and M739E mutants prior to any oxidant application were shifted to more hyperpolarized voltages (Table 3; 140.7 ± 4.0 and 109.6 ± 2.6 mV, respectively; $n = 5$) compared with that of wild-type hSlo1 (~170 mV), practically functioning as if they had been already oxidized by Ch-T. Moreover, treatment with Ch-T did not appreciably shift the *G–V* curve (Fig. 6*A*) or slow the deactivation kinetics (Fig. 6*B* and *C*) in the mutants M712E or M739E (Tables 3 and 4). In contrast, the M536E mutant maintained the characteristic increase in open probability and slowed deactivation following application of Ch-T, indicating that the hydrophilic property of met-O at this position does not account for the functional changes. Taken together, these results suggest that disruption of the hydrophobic environment surrounding M712 or M739 may account for the ability of met-O at those locations to cause the functional effects of oxidation, whereas oxidative modification of M536 may ultimately lead to structural changes within the channel by a different mechanism.

Ch-T effects disappear with increasing $[Ca^{2+}]_i$

To assess how methionine oxidation alters the Ca^{2+}-dependent gating of hSlo1, we examined the Ch-T sensitivity in a broad range of $[Ca^{2+}]_i$, including 5 μM and 120 μM. The former concentration is within the range of the K_D values of the mSlo1 Ca^{2+} binding sites, which vary depending on the states of the intrinsic gate and the voltage sensors (Horrigan & Aldrich, 2002). At the latter concentration, the high-affinity Ca^{2+} sites are probably saturated (Cox *et al.* 1997; Zhang *et al.* 2001; Zeng *et al.* 2005). The *G–V* curves at these $[Ca^{2+}]_i$ levels and the resulting Ca^{2+} dependence of $V_{0.5}$, which is an approximate measure of the overall Ca^{2+} dependence, before and after treatment with Ch-T are shown in Fig. 7*B*. The wild-type hSlo1 Ch-T effects were conspicuous at 0 and 200 nM $[Ca^{2+}]_i$, but absent at both 5 μM and 120 μM (Fig. 7*A*). The Triple Met mutant retained Ca^{2+}-dependent activation indistinguishable from that of the wild-type channel, such that 120 μM $[Ca^{2+}]_i$ also represented a saturating concentration for this mutant channel with 200 μM $[Ca^{2+}]_i$ failing to

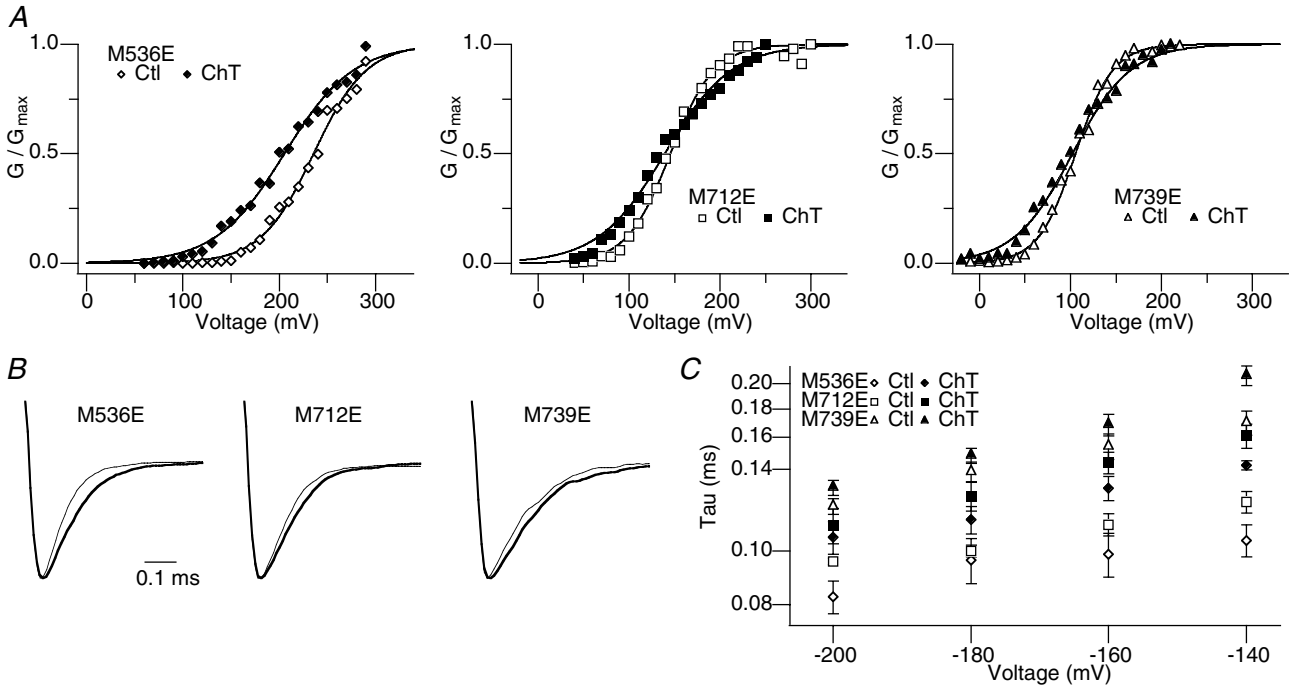

Figure 6. Substitution of M712 or M739 with glutamate mimics oxidation
A, representative M536E (left), M712E (middle), and M739E (right) *G–V* curves before (open symbols) and after (filled symbols) treatment with Ch-T. See Table 3 for mean ± S.E.M. values; $n = 5$. *B*, M536E (left), M712E (middle), and M739E (right) scaled tail currents recorded at −200 mV after pulses to 180 mV before (thin sweep) and after (thick sweep) Ch-T modification. *C*, voltage dependence of the deactivation time constant for M536E (diamonds), M712E (squares), and M739E (triangles) before (open symbols) and after (filled symbols) application of Ch-T. See Table 4 for mean ± S.E.M. values.

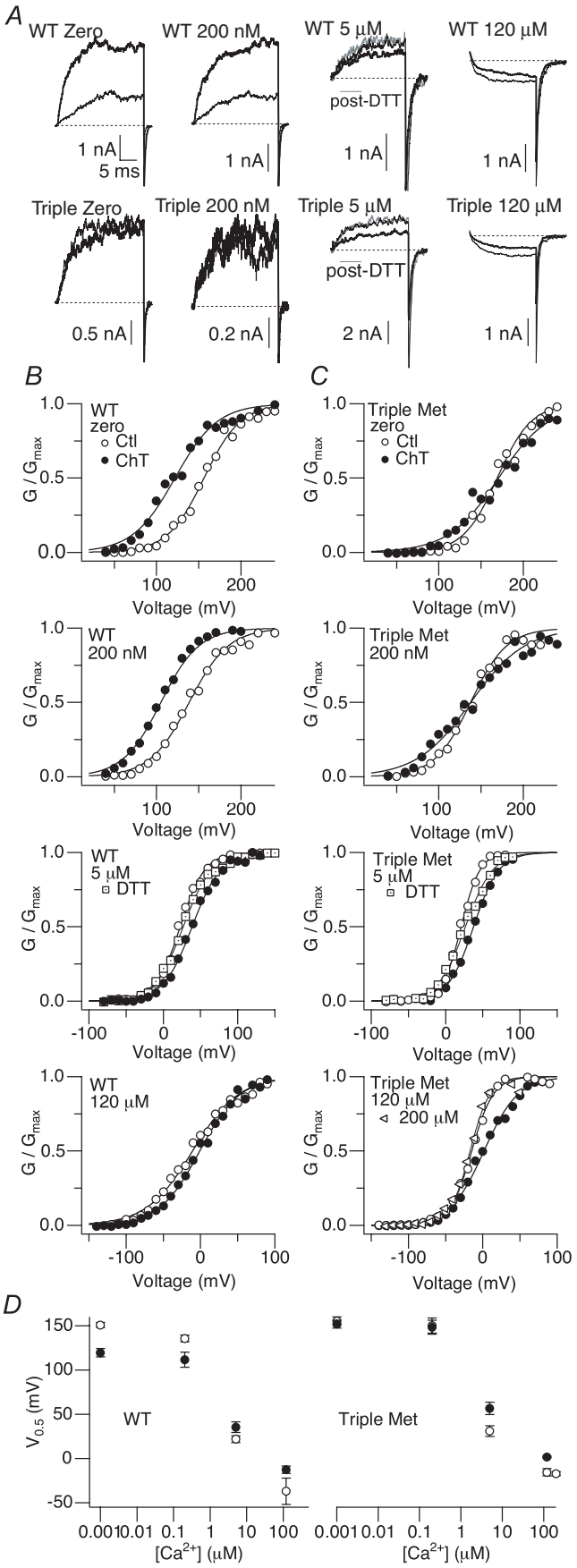

produce a greater effect on open probability (Fig. 7*C*). Furthermore, unlike the wild-type hSlo1 results, oxidative modification did not shift the $V_{0.5}$ of Triple Met to more hyperpolarized voltages at any of the $[Ca^{2+}]_i$ concentrations (Fig. 7*D*). Small decreases in the open probability of both the wild-type and mutant channels at 5 μM and 120 μM $[Ca^{2+}]_i$ following treatment with Ch-T were readily reversed by the reducing agent DTT, suggesting that cysteine oxidation may have contributed to the observations at these high $[Ca^{2+}]_i$ values (Tang *et al.* 2004).

Simulation of the Ch-T effect on hSlo1 *G–V* curves

Gating of the Slo1 channel, which involves allosteric interactions among its intrinsic gate, voltage sensors and divalent cation binding sites, is well approximated by the HA model (Fig. 8*Aii*) (Horrigan & Aldrich, 2002), which incorporates Ca^{2+} into the earlier HCA model (Fig. 8*Ai*) (Horrigan *et al.* 1999). These biophysical models provide a framework to examine the effects of Ca^{2+} binding

Figure 7. The effect of Ch-T on channel open probability depends on $[Ca^{2+}]$

A, representative wild-type hSlo1 (top) and Triple Met mutant (bottom) currents before (thin sweep) and after (thick sweep) Ch-T treatment. The zero, 200 nM, 5 μM, and 120 μM $[Ca^{2+}]_i$ currents were elicited in response to pulses from 0 to 120 mV, 0 to 100 mV, −80 to 20 mV, and −130 to −20 mV, respectively. Grey sweeps denote currents in 5 μM $[Ca^{2+}]_i$ post-DTT treatment. Dotted lines represent the zero current level. *B*, representative wild-type hSlo1 *G–V* curves before (○) and after (●) modification by Ch-T. Currents were first elicited by pulsing to different test potentials in the virtual absence of Ca^{2+}. This recording protocol was repeated after bath application of 200 nM, 5 μM, or 120 μM Ca^{2+}. Tail currents in zero, 200 nM, 5 μM, and 120 μM $[Ca^{2+}]_i$ were measured at −50, −50, −80, and −120 mV, respectively. Following a return to zero Ca^{2+} for treatment with 2 mM Ch-T, the recording protocols were again repeated in zero and then the appropriate $[Ca^{2+}]_i$. The zero, 200 nM, 5 μM and 120 μM $[Ca^{2+}]_i$ mean $V_{0.5}$ values for the results obtained before and after Ch-T application were 150.8 ± 2.8 and 119.6 ± 4.4 mV ($\Delta V_{0.5} = -31.2$ mV), 135.5 ± 3.8 and 111.7 ± 2.9 mV ($\Delta V_{0.5} = -23.8$ mV), 21.8 ± 3.9 and 35.3 ± 2.6 mV ($\Delta V_{0.5} = 13.5$ mV), and −36.9 ± 15 and −2.6 ± 11 mV ($\Delta V_{0.5} = 24.3$ mV), respectively. The 5 μM $[Ca^{2+}]_i$ mean $V_{0.5}$ value obtained after DTT (dotted squares) application was 32.3 ± 2.8 mV ($\Delta V_{0.5} = 10.5$ mV). *C*, representative Triple Met mutant *G–V* curves before (○) and after (●) treatment with Ch-T. The recording protocol was identical to that in *B*. The 0, 200 nM, 5 μM and 120 μM $[Ca^{2+}]_i$ mean $V_{0.5}$ values for the results obtained before and after Ch-T application were 155.2 ± 4.7 and 151.7 ± 4.5 mV ($\Delta V_{0.5} = -3.5$ mV), 150.3 ± 8.4 and 148.2 ± 7.8 mV ($\Delta V_{0.5} = -2.1$ mV), 31.0 ± 5.9 and 56.7 ± 7.1 mV ($\Delta V_{0.5} = 25.7$ mV), and −15.6 ± 4.0 and 1.6 ± 1.1 mV ($\Delta V_{0.5} = 17.2$ mV), respectively. The 5 μM $[Ca^{2+}]_i$ mean $V_{0.5}$ value obtained after DTT (dotted squares) application was 40.4 ± 7.9 mV ($\Delta V_{0.5} = 9.4$ mV). The 200 μM $[Ca^{2+}]_i$ control mean $V_{0.5}$ value (open sideways triangles) was −17.1 ± 2.1 mV. *D*, wild-type hSlo1 (left) and Triple Met (right) $V_{0.5}$ values before (○) and after (●) treatment with Ch-T at different concentrations of $[Ca^{2+}]_i$. The symbols for Triple Met in the control condition may be located directly under those of the Ch-T condition. The error bars in some cases are smaller than the symbol size ($n = 3$).

A

	Control	Ch-T	Fold Change
Equilibrium Constant L_0	5.0E-06	2.0E-05	4
Equilibrium Constant J	0.042	0.11	2.6
Allosteric Factor D	11	8	0.73
Allosteric Factor C	10	5	0.5

i. HCA model

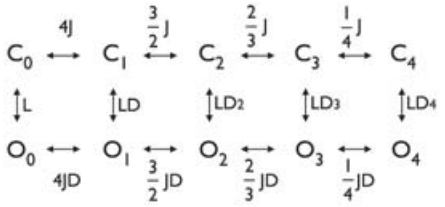

ii. HA model

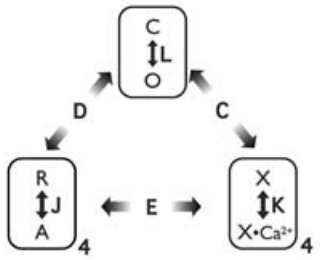

B

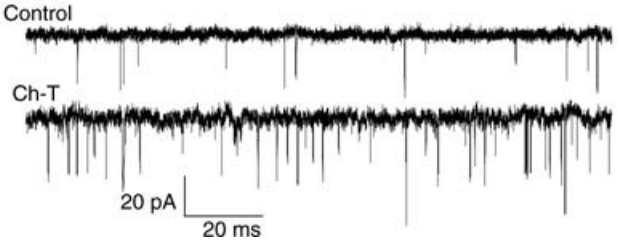

C

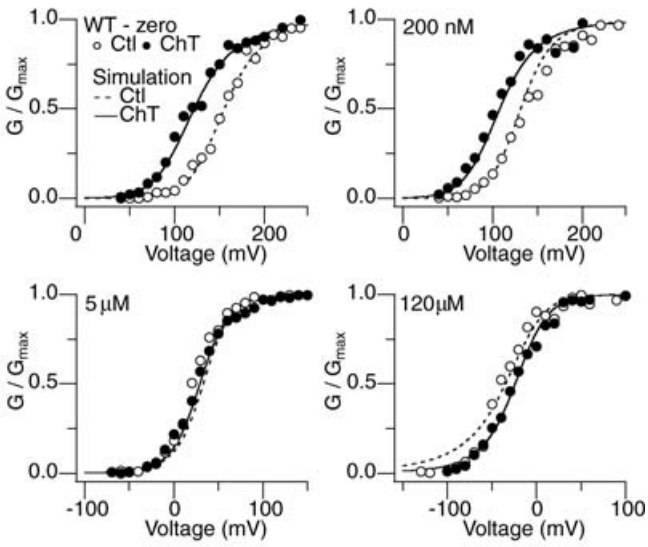

D

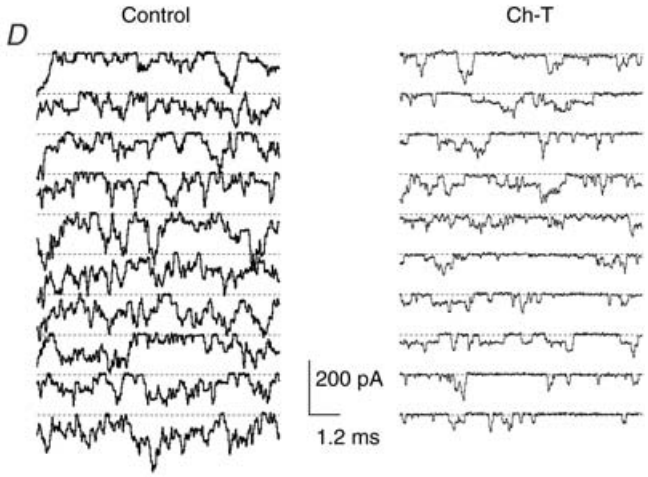

Figure 8. Simulation of the Ch-T effect on hSlo1 function at various [Ca^{2+}] using the HA model
A, the model parameters adjusted to account for the changes in hSlo1 function at ~0, 200 nM, 5 μM and 120 μM $[Ca^{2+}]_i$ caused by treatment with Ch-T. The HCA model used to analyse low Ca^{2+} data is shown using equilibrium constants (i) and the HA model, an extension of the HCA model incorporating Ca^{2+}-binding events, is depicted below (ii). The HA diagram includes three allosteric components: the intrinsic pore opening and closing (top), four voltage sensors (bottom left) and four Ca^{2+} binding segments (bottom right). The pore is either closed (C) or open (O), each voltage sensor is at rest (R) or activated (A), and each Ca^{2+} binding site is empty (X) or occupied by Ca^{2+} (X•Ca^{2+}). The allosteric interaction factors D, C and E specify the extent of interactions among the three allosteric components. The HCA model (i, top), a subset of the HA model, does not consider Ca^{2+} binding and the equilibrium constants J and L and the allosteric interaction factor D are as in the HA model. The equilibrium constant L_0 represents L at 0 mV. *B*, representative channel openings from a single patch in 0 $[Ca^{2+}]_i$ at −150 mV in the control condition (top) and after modification by Ch-T (bottom). Downward deflections represent opening transitions. The mean open probability before and after Ch-T was 0.0018 ± 0.0006 and 0.0083 ± 0.004, respectively ($n = 5$). The mean open duration before and after oxidation was 0.066 ± 0.007 and 0.083 ± 0.002 ms, respectively. *C*, simulated *G–V* curves before (dashed lines) and after (thick lines) application of Ch-T superimposed upon experimental *G–V* curves before (○) and after (●) oxidation. The data presented in the 5 μM $[Ca^{2+}]_i$ post-Ch-T condition corresponds to treatment after both Ch-T and DTT to remove the unwanted influence of cysteine oxidation at high $[Ca^{2+}]_i$. Simulated curves representing the control condition were generated with parameter values similar to those of the HA model except for the following changes which better described the data: D = 11 (from 11.6) and C = 10

and other modulatory influences on the gating process (Tang *et al.* 2001; Santarelli *et al.* 2004; Horrigan *et al.* 2005). While many states are formally present in the HA model, estimation of the parameter values in the model is facilitated by measurements taken at extreme voltages and/or Ca^{2+} levels to functionally isolate subsets of the gating behaviour. For example, the intrinsic gating of the channel pore without any influence from the voltage sensors or Ca^{2+} binding sites, denoted as the equilibrium constant L_0 in the HCA and HA models, may be inferred from the single-channel measurements at very negative voltages (−150 mV) without Ca^{2+} (Fig. 8*B*). Under such conditions, we found that treatment with Ch-T increased the open probability by ∼4-fold and increased the mean open duration by ∼25% ($n = 5$).

Tang *et al.* (2001) simulated the leftward shift of the *G–V* curve following treatment with Ch-T in low $[Ca^{2+}]_i$ by increasing the highly voltage-dependent equilibrium constant J. We implemented a similar increase in J, along with the increase in L_0 and a 30% decrease in the parameter D, which describes the allosteric interaction between the voltage sensors and the pore, to account for the *G–V* slope change (ΔQ_{app}) following oxidation, which is statistically absent from that of the Triple Met mutant. However, these three changes were not sufficient to reproduce the effect of oxidation by Ch-T over a wide range of voltages and $[Ca^{2+}]_i$ because such changes predict that the leftward shift of *G–V* persists even at saturating levels of Ca^{2+} (e.g. ≥ 100 μM; see Fig. 7). The Ca^{2+} dependence of the Ch-T effect was simulated by decreasing the value of the parameter C, which describes the allosteric interaction between Ca^{2+} binding and opening of the pore, by 50%. This change in C in conjunction with the experimentally measured increase in L_0 (Fig. 8*B*) and the changes in J and D (Fig. 8*A*) successfully simulate the Ch-T-induced changes in *G–V* over the entire range of $[Ca^{2+}]_i$, from 0 to 120 μM (Fig. 8*C*).

The decrease in the allosteric factor C implemented in our simulation was experimentally corroborated in the following manner. According to the HA model, the Slo1 channel activity at extreme negative voltages in the presence of saturating $[Ca^{2+}]_i$ is described by $L_0{*}C^4$ as the model assumes four subunits. If the value of C decreases, as suggested by our simulation, the channel activity should decrease following treatment with Ch-T. Consistent with this prediction, the open probability of the wild-type hSlo1 channel at −160 mV and 120 μM $[Ca^{2+}]_i$ did markedly decrease by ∼2-fold following treatment with Ch-T, as exemplified by the single-channel measurements shown in Fig. 8*D*. We do note, however, that the decrease in open probability observed is generally smaller than predicted by the simulation results.

Discussion

M536, M712 and M739 specifically confer oxidative sensitivity to hSlo1

Methionine oxidation within hSlo1 consistently leads to a marked increase in the channel open probability and slowing of deactivation within the physiologically relevant voltage range in isolated membrane patches at low $[Ca^{2+}]_i$ (Tang *et al.* 2001; Santarelli *et al.* 2004). Here, we demonstrate that these functional effects of methionine oxidation are mediated by M536, M712 and M739 located in the cytoplasmic RCK1–RCK2 domains. Contemporaneous mutation of these three specific methionine residues to leucine eliminates the hallmark leftward shift of the *G–V* curve and the slowing of deactivation caused by the oxidant Ch-T. Neither conservative mutation of single methionine residues throughout hSlo1 nor mutations of any two of these three key methionine residues abolishes or even reduces the functional sensitivity to the oxidant. Furthermore, this set of three residues is unique in that channels comprised of different assortments of three closely related methionine-to-leucine mutations maintain the typical oxidative sensitivity; however, the effectiveness of a vastly different, alternative mutation combination, though unlikely, cannot be formally excluded.

The concurrent mutation of M536, M712 and M739 to leucine is required to eliminate the oxidative sensitivity because the modification of only one of these key methionine residues is sufficient to generate the functional effects following oxidation by Ch-T. Hence, our results under these conditions do not readily support an additive type of oxidative sensitivity, whereby each of the three methionine residues contributes a small fixed portion of the Ch-T sensitivity to the channel so that only when all three are oxidized is the sensitivity detectable. Indeed, the oxidative sensitivities of the single and double methionine mutants are not significantly less than that of the wild-type channel. Furthermore, the idea that the triple methionine-to-leucine mutation hinders the access of Ch-T to the true single-methionine target elsewhere can be rejected because none of the single methionine point mutants demonstrated a loss in Ch-T sensitivity. The ability of any one of the three critical methionine

(from 8). Simulated curves representing the Ch-T condition were produced from the model following the alterations shown in *A*. *D*, representative channel openings from a single patch in 120 μM $[Ca^{2+}]_i$ at −160 mV in the control condition (left) and after modification by Ch-T (right). Downward deflections represent opening transitions. The individual sweep duration was shorter than that exhibited in *B* in order to maintain patch stability with high $[Ca^{2+}]_i$.

residues to cause the functional changes observed predicts that the oxidative modification kinetics of the single- and double-mutant channels be slower than that of the wild-type hSlo1 channel because the mutants have fewer targets. However, our results failed to reveal any measurable difference in the modification kinetics among the mutant and wild-type channels.

The results presented here demonstrate that the sensitivity to methionine oxidation is conferred by the presence of at least one of the three critical methionine residues in Slo1. Since four Slo1 subunits form one functional complex (Shen *et al.* 1994), each Slo1 channel in turn contains 12 potential target methionine residues. How the targets in the four subunits interact to cause the observed electrophysiological consequences remains to be investigated.

β1 does not fully recover the functional effects of oxidation lost to mutation

Expression of auxiliary subunits with mutant ion channels is often utilized as a tool to better understand the effects of a mutation and to determine whether a functional alteration by the mutation can be rescued (Nuss *et al.* 1996; Qian & Magleby, 2003; Hatano *et al.* 2004). For instance, near-normal Ca^{2+} sensitivity is restored in an otherwise Ca^{2+}-insensitive Slo1 channel by coexpression with β1 (Qian & Magleby, 2003). However, our results show that β1 does not restore the characteristic Ch-T sensitivity observed in the wild-type Slo1 + β1 complex (i.e. −75 mV shift in $V_{0.5}$ and substantial slowing of deactivation) to the Triple Met mutant that is functionally insensitive to methionine oxidation. Although the Triple Met + β1 does not show any slowing of deactivation following treatment with Ch-T, the cause of the small residual shift in $V_{0.5}$ observed is unknown. Perhaps an additional, albeit less effective, oxidation target site within the pore-forming portion of the channel complex may become exposed for modification and/or only influence the open probability, but not deactivation, within the presence of β1.

HA model-based interpretations

Tang *et al.* (2001) simulated hSlo1 currents recorded in the absence of $[Ca^{2+}]_i$ before and after oxidation with Ch-T using the HCA model (Horrigan *et al.* 1999). The HCA model equilibrium constant J, pertaining to the steeply voltage-dependent transitions that most probably reflect the voltage-sensor movements, was increased by approximately 2-fold to account for the leftward shift in *G–V*. Whereas that strategy required a change in only one model parameter to account for most of the observed change in $V_{0.5}$ in the absence of $[Ca^{2+}]_i$, the results presented in this study clearly show that the change in J must be accompanied by alterations in additional model parameters to adequately describe the functional effects of methionine oxidation over wide ranges of voltage and $[Ca^{2+}]_i$.

The Slo1 channel behaviour in the presence of $[Ca^{2+}]_i$ is successfully described by the HA model (Horrigan & Aldrich, 2002), which builds on the HCA model by incorporating Ca^{2+} binding as an additional allosteric dimension (see also Rothberg & Magleby, 2000). Using the HA model, we have demonstrated here that changes in three other parameters, in addition to J, more accurately simulate the functional effects of methionine oxidation in hSlo1. At −150 mV in the virtual absence $[Ca^{2+}]_i$, where the voltage-sensor and Ca^{2+}-mediated activation of the channel is negligible, methionine oxidation significantly enhances the open probability, which in turn suggests that oxidation alters the equilibrium constant L_0 that describes the intrinsic pore gate behaviour. However, changes in L_0 and J do not satisfactorily reproduce the observed decrease in the steepness of the *G–V* slope or the lack of a leftward shift of the *G–V* curve in high $[Ca^{2+}]_i$. Indeed, decreases in the values of the allosteric factors D and C, along with the alterations in J and L_0, successfully simulate the functional outcomes of methionine oxidation in hSlo1 (Fig. 8).

The way in which oxidation of M536, M712 or M739 in the cytoplasmic RCK domains affects channel function may be similar to the mechanism that has been proposed to explain how Ca^{2+} binding affects the shape of the gating ring to promote opening of the Slo channel (Jiang *et al.* 2002; Niu *et al.* 2004). Both processes increase the open probability of the channel; however, the effects of Ca^{2+} binding and methionine oxidation on the open probability are additive only at low to moderate $[Ca^{2+}]_i$. At high $[Ca^{2+}]_i$, the increase in the open probability following oxidation is no longer present. This Ca^{2+} dependence is accounted for in our simulations by a decrease in the strength of allosteric coupling between Ca^{2+} binding and the movement of the channel gate reflected in the allosteric coupling factor C in the HA model. Thus, our simulations suggest that oxidation of M536, M712 or M739 in hSlo1 renders the channel less sensitive to Ca^{2+} (smaller C), which would shift $V_{0.5}$ to the more positive direction in a Ca^{2+}-dependent manner, but that this inhibitory effect on open probability is counteracted by the oxidative enhancement of the voltage-sensor-mediated gating (greater J) and the intrinsic gating (greater L_0).

Horrigan *et al.* (2005) analysed the action of intracellular heme on the Slo1 BK channel using the HA model and found that heme increases L_0 and decreases D and C in the model. The same HA model parameters are also affected by methionine oxidation within hSlo1 in a similar manner. Thus, as suggested by Horrigan *et al.* (2005) to explain the heme action, we postulate that the L_0 increase reflects a partial expansion of the gating-ring complex when the pore gate is closed to favour

the open state of the channel. The decreases in D and C probably represent the less-than-normal expansion of the gating-ring complex when the pore gate is open. How oxidation of the methionine residues in hSlo1 increases J is less certain. If the oxidation alters the interaction between the voltage sensor and the gating-ring complex to favour the activated state of the voltage sensor irrespective of the pore gate status, then the value of the parameter J is expected to increase.

Physical mechanisms

The physical mechanism by which oxidation of M536, M712 or M739 in the cytoplasmic domain of hSlo1 causes the postulated changes in the behaviour of the gating-ring complex and the voltage sensors in hSlo1 can only be conjectured. Comparison of the amino-acid sequences of hSlo1 and the bacterial channel MthK whose crystallographic structure is known (Jiang *et al.* 2002) suggests M536 is located within the RCK1 domain near the flexible interface and closer to the transmembrane domain (Jiang *et al.* 2001, 2002), while M712 and M739 may be located at relatively more distant sites in the probable RCK2 domain. We postulate that the side chains of M712 and M739 may be situated within close proximity in a relatively hydrophobic environment in part because introduction of the hydrophilic amino acid glutamate at either of the two positions mimics oxidative treatment and essentially removes oxidant sensitivity. Thus, oxidation of either of the two residues to met-O, making the side chain much more polar and comparable to lysine (Black & Mould, 1991), may lead to repulsion between the side chains of the met-O and nearby non-polar residues or repositioning to expose the met-O to water, thereby disrupting the normally hydrophobic milieu. Any resulting structural or energetic changes due to the oxidation could then be coupled to the channel's pore gate.

If the oxidative effects at M712 and M739 do not directly affect the pore, then a good candidate for coupling such functional changes in the channel might be M536, which is probably located on the flexible interface of the RCK1 domain (Jiang *et al.* 2001, 2002). The presence of methionine at position 536 in the RCK1 domain confers full oxidative sensitivity for the channel, as demonstrated by the robust Ch-T sensitivity in the double mutant M712L–M739L. Therefore, we suggest that oxidation of M536 fully reproduces the changes induced by oxidation of M712 and M739 to met-O in the RCK2 domain. However, in contrast to the mechanism proposed for modification of M712 or M739 that relies on the change from a hydrophobic to hydrophilic residue, changes in hydrophobicity at position 536 are unlikely to be critical because the M536E channel retains noticeable oxidant sensitivity. Instead, the increased rigidity of the met-O side chain as compared with that of methionine may alter the local structure of the flexible interface near M536, ultimately affecting the position of the pore gate.

In the absence of a high-resolution structure of the hSlo1 channel and additional functional information, alternative models to account for the mechanism of action of methionine oxidation on Slo1 channel function are possible. Nevertheless, the concurrent mutation of M536, M712 and M739 removes the methionine-directed oxidative sensitivity from hSlo1. Although the physical bases for the roles played by M536 and M712/M739 are probably different, the functional outcomes due to their modification are indistinguishable and not additive in nature.

Physiological implications

The individual ability of not one, but three specific methionine residues in hSlo1, to generate the complete functional effects of methionine oxidation suggests substantial evolutionary and adaptive significance. Indeed, M536, M712 and M739 are well conserved in the fly, mouse, rat and human Slo1 channels. Any modulation of the Slo1 channel activity will clearly influence vital physiological processes given its abundant expression in vascular smooth muscle and brain, and crucial contributions to smooth muscle tone and neuronal excitability. With a greater role being assigned to oxidants as signal transduction messengers and the reversible nature of methionine oxidation, the Slo1 channel may be a critical component in oxidation-sensitive signalling cascades.

The obvious increase in open probability and slowed deactivation following methionine oxidation of the channel at low $[Ca^{2+}]_i$ indicates that oxidation within hSlo1 may serve as a protective mechanism by allowing for a greater degree of potassium efflux, consequently favouring the resting or inactive state of the cell. This role would be particularly advantageous at pathological times of assault by increased levels of reactive oxygen species, such as those associated with reperfusion following ischaemia or during neurodegenerative disease, when heightened cellular activity has been shown to lead to cell death (Halliwell, 1992; Lipton, 1999; Agar & Durham, 2003). Under such stress conditions, the Ca^{2+}-dependent activation of BK channels may act as a feedback mechanism to prevent excitotoxicity. In contrast, increased activation of the channels facilitated by methionine oxidation at low $[Ca^{2+}]_i$ where the channels do have a relatively low open probability under physiological conditions may serve as a pre-emptive feed-forward mechanism of cell protection. Furthermore, restriction of the oxidative effects to low $[Ca^{2+}]_i$ may be beneficial. Indeed, an hSlo1 genetic mutation that increases open probability in a wide range of $[Ca^{2+}]_i$ by increasing the Ca^{2+} sensitivity by 3- to 5-fold has been shown to underlie inherited, coexisting generalized epilepsy and paroxysmal dyskinesia (Du *et al.*

2005). Therefore, the lack of a further increase in open probability due to methionine-directed oxidation at high $[Ca^{2+}]_i$ may in fact be vital.

Pharmacologically enhanced opening of BK channels located within cardiac mitochondria, where reactive oxygen species are produced, confers a preconditioning role that significantly reduces infarct size following ischaemic injury in the heart (Xu *et al.* 2002; Sato *et al.* 2005). Similarly, in the brain, modulation of BK channel activity influences the extent of cell degeneration following ischaemia, with blockade of the channels exacerbating the detrimental effects of the glutamate toxicity (Runden-Pran *et al.* 2002). In addition, oxidation has been shown to reduce hippocampal susceptibility to hypoxia-induced spreading of anoxic depolarization via the activation of BK channels (Hepp *et al.* 2005). These aforementioned examples strongly suggest that methionine oxidation of the BK channel may indeed be cell protective.

In summary, we have demonstrated that three specific hSlo1 methionine residues (M536, M712 and M739) confer oxidative sensitivity to the channel. Oxidation of at least one of these methionine residues causes an increase in the open probability of the channel and a slowing of deactivation in low $[Ca^{2+}]_i$, though these functional effects are not evident at saturating $[Ca^{2+}]_i$. Oxidants are known to cause alteration in protein function, but the precise molecular targets for oxidation and the mechanism by which the modification ultimately leads to the functional changes remain largely obscure. Hence, methionine oxidation within the hSlo1 channel may be one of a handful of examples (Ciorba *et al.* 1997) where these goals have been realized. Whether methionine-specific oxidation of the Slo channel occurs *in vivo* remains to be determined. However, explicit targeting of methionine residues in the channel may provide a new approach to enhance BK channel activity and thereby significantly impact the state of the cell during normal homeostasis and oxidative stress.

References

Agar J & Durham H (2003). Relevance of oxidative injury in the pathogenesis of motor neuron diseases. *Amyotroph Lateral Scler Other Motor Neuron Disord* **4**, 232–242.

Avdonin V, Tang XD & Hoshi T (2003). Stimulatory action of internal protons on Slo1 BK channels. *Biophys J* **84**, 2969–2980.

Black SD & Mould DR (1991). Development of hydrophobicity parameters to analyze proteins which bear post- or cotranslational modifications. *Anal Biochem* **193**, 72–82.

Brenner R, Perez GJ, Bonev AD, Eckman DM, Kosek JC, Wiler SW, Patterson AJ, Nelson MT & Aldrich RW (2000). Vasoregulation by the β1 subunit of the calcium-activated potassium channel. *Nature* **407**, 870–876.

Chen J, Avdonin V, Ciorba MA, Heinemann SH & Hoshi T (2000). Acceleration of P/C-type inactivation in voltage-gated K^+ channels by methionine oxidation. *Biophys J* **78**, 174–187.

Ciorba MA, Heinemann SH, Weissbach H, Brot N & Hoshi T (1997). Modulation of potassium channel function by methionine oxidation and reduction. *Proc Natl Acad Sci U S A* **94**, 9932–9937.

Ciorba MA, Heinemann SH, Weissbach H, Brot N & Hoshi T (1999). Regulation of voltage-dependent K^+ channels by methionine oxidation: effect of nitric oxide and vitamin C. *FEBS Lett* **442**, 48–52.

Cox DH, Cui J & Aldrich RW (1997). Allosteric gating of a large conductance Ca-activated K^+ channel. *J General Physiol* **110**, 257–281.

Dichiara TJ & Reinhart PH (1997). Redox modulation of hslo Ca^{2+}-activated K^+ channels. *J Neurosci* **17**, 4942–4955.

Du W, Bautista JF, Yang H, Diez-Sampedro A, You SA, Wang L, Kotagal P, Luders HO, Shi J, Cui J, Richerson GB & Wang QK (2005). Calcium-sensitive potassium channelopathy in human epilepsy and paroxysmal movement disorder. *Nat Genet* **37**, 733–738.

Evans MD & Pryor WA (1994). Cigarette smoking, emphysema, and damage to alpha 1-proteinase inhibitor. *Am J Physiol* **266**, L593–L611.

Gao J, Yin DH, Yao YH, Sun HY, Qin ZH, Schoneich C, Williams TD & Squier TC (1998). Loss of conformational stability in calmodulin upon methionine oxidation. *Biophys J* **74**, 1115–1134.

Halliwell B (1992). Reactive oxygen species and the central nervous system. *J Neurochem* **59**, 1609–1623.

Hatano N, Ohya S, Muraki K, Clark RB, Giles WR & Imaizumi Y (2004). Two arginines in the cytoplasmic C-terminal domain are essential for voltage-dependent regulation of A-type K^+ current in the Kv4 channel subfamily. *J Biol Chem* **279**, 5450–5459.

Hepp S, Gerich FJ & Muller M (2005). Sulfhydryl oxidation reduces hippocampal susceptibility to hypoxia-induced spreading depression by activating BK channels. *J Neurophysiol* **94**, 1091–1103.

Horrigan FT & Aldrich RW (2002). Coupling between voltage sensor activation, Ca^{2+} binding and channel opening in large conductance (BK) potassium channels. *J General Physiol* **120**, 267–305.

Horrigan FT, Cui J & Aldrich RW (1999). Allosteric voltage gating of potassium channels I. mSlo ionic currents in the absence of Ca^{2+}. *J General Physiol* **114**, 277–304.

Horrigan FT, Heinemann SH & Hoshi T (2005). Heme regulates allosteric activation of the Slo1 BK channel. *J General Physiol* **126**, 7–21.

Houghten RA & Li CH (1976). Studies on pituitary prolactin. 39. Reaction of the ovine hormone with hydrogen peroxide. *Biochim Biophys Acta* **439**, 240–249.

Hu H, Shao LR, Chavoshy S, Gu N, Trieb M, Behrens R, Laake P, Pongs O, Knaus HG, Ottersen OP & Storm JF (2001). Presynaptic Ca^{2+}-activated K^+ channels in glutamatergic hippocampal terminals and their role in spike repolarization and regulation of transmitter release. *J Neurosci* **21**, 9585–9597.

Jaggar JH, Porter VA, Lederer WJ & Nelson MT (2000). Calcium sparks in smooth muscle. *Am J Physiol Cell Physiol* **278**, C235–C256.

Jiang Y, Lee A, Chen J, Cadene M, Chait BT & MacKinnon R (2002). Crystal structure and mechanism of a calcium-gated potassium channel. *Nature* **417**, 515–522.

Jiang Y, Pico A, Cadene M, Chait BT & MacKinnon R (2001). Structure of the RCK domain from the *E. coli* K^+ channel and demonstration of its presence in the human BK channel. *Neuron* **29**, 593–601.

Jiang Z, Wallner M, Meera P & Toro L (1999). Human and rodent MaxiK channel beta-subunit genes: cloning and characterization. *Genomics* **55**, 57–67.

Johnson D & Travis J (1979). The oxidative inactivation of human alpha-1-proteinase inhibitor. Further evidence for methionine at the reactive center. *J Biol Chem* **254**, 4022–4026.

Levine RL, Mosoni L, Berlett BS & Stadtman ER (1996). Methionine residues as endogenous antioxidants in proteins. *Proc Natl Acad Sci U S A* **93**, 15036–15040.

Lipton P (1999). Ischemic cell death in brain neurons. *Physiol Rev* **79**, 1431–1568.

Long SB, Campbell EB & Mackinnon R (2005). Crystal structure of a mammalian voltage-dependent Shaker family K^+ channel. *Science* **309**, 897–903.

Meera P, Wallner M, Song M & Toro L (1997). Large conductance voltage- and calcium-dependent K^+ channel, a distinct member of voltage-dependent ion channels with seven N-terminal transmembrane segments (S0–S6), an extracellular N terminus, and an intracellular (S9–S10) C terminus. *Proc Natl Acad Sci U S A* **94**, 14066–14071.

Meredith AL, Thorneloe KS, Werner ME, Nelson MT & Aldrich RW (2004). Overactive bladder and incontinence in the absence of the BK large conductance Ca^{2+}-activated K^+ channel. *J Biol Chem* **279**, 36746–36752.

Moskovitz J, Bar-Noy S, Williams WM, Requena J, Berlett BS & Stadtman ER (2001). Methionine sulfoxide reductase (MsrA) is a regulator of antioxidant defense and lifespan in mammals. *Proc Natl Acad Sci U S A* **98**, 12920–12925.

Nelson MT, Cheng H, Rubart M, Santana LF, Bonev AD, Knot HJ & Lederer WJ (1995). Relaxation of arterial smooth muscle by calcium sparks. *Science* **270**, 633–637.

Niu X & Magleby KL (2002). Stepwise contribution of each subunit to the cooperative activation of BK channels by Ca^{2+}. *Proc Natl Acad Sci U S A* **99**, 11441–11446.

Niu X, Qian X & Magleby KL (2004). Linker-gating ring complex as passive spring and Ca^{2+}-dependent machine for a voltage- and Ca^{2+}-activated potassium channel. *Neuron* **42**, 745–756.

Nuss HB, Balser JR, Orias DW, Lawrence JH, Tomaselli GF & Marban E (1996). Coupling between fast and slow inactivation revealed by analysis of a point mutation (F1304Q) in μ1 rat skeletal muscle sodium channels. *J Physiol* **494**, 411–429.

Qian X & Magleby KL (2003). Beta1 subunits facilitate gating of BK channels by acting through the Ca^{2+}, but not the Mg^{2+}, activating mechanisms. *Proc Natl Acad Sci U S A* **100**, 10061–10066.

Roosild TP, Le KT & Choe S (2004). Cytoplasmic gatekeepers of K^+-channel flux: a structural perspective. *Trends Biochem Sci* **29**, 39–45.

Rothberg BS & Magleby KL (2000). Voltage and Ca^{2+} activation of single large-conductance Ca^{2+}-activated K^+ channels described by a two-tiered allosteric gating mechanism. *J General Physiol* **116**, 75–99.

Runden-Pran E, Haug FM, Storm JF & Ottersen OP (2002). BK channel activity determines the extent of cell degeneration after oxygen and glucose deprivation: a study in organotypical hippocampal slice cultures. *Neuroscience* **112**, 277–288.

Santarelli LC, Chen J, Heinemann SH & Hoshi T (2004). The β1 subunit enhances oxidative regulation of large-conductance calcium-activated K^+ channels. *J General Physiol* **124**, 357–370.

Sato T, Saito T, Saegusa N & Nakaya H (2005). Mitochondrial Ca^{2+}-activated K^+ channels in cardiac myocytes: a mechanism of the cardioprotective effect and modulation by protein kinase A. *Circulation* **111**, 198–203.

Sausbier M, Arntz C, Bucurenciu I, Zhao H, Zhou XB, Sausbier U *et al.* (2005). Elevated blood pressure linked to primary hyperaldosteronism and impaired vasodilation in BK channel-deficient mice. *Circulation* **112**, 60–68.

Sausbier M, Hu H, Arntz C, Feil S, Kamm S, Adelsberger H *et al.* (2004). Cerebellar ataxia and Purkinje cell dysfunction caused by Ca^{2+}-activated K^+ channel deficiency. *Proc Natl Acad Sci U S A* **101**, 9474–9478.

Shao LR, Halvorsrud R, Borg-Graham L & Storm JF (1999). The role of BK-type Ca^{2+}-dependent K^+ channels in spike broadening during repetitive firing in rat hippocampal pyramidal cells. *J Physiol* **521**, 135–146.

Shen KZ, Lagrutta A, Davies NW, Standen NB, Adelman JP & North RA (1994). Tetraethylammonium block of Slowpoke calcium-activated potassium channels expressed in *Xenopus* oocytes: evidence for tetrameric channel formation. *Pflugers Arch* **426**, 440–445.

Soto MA, Gonzalez C, Lissi E, Vergara C & Latorre R (2002). Ca^{2+}-activated K^+ channel inhibition by reactive oxygen species. *Am J Physiol Cell Physiol* **282**, C461–C471.

Stadtman ER, Moskovitz J & Levine RL (2003). Oxidation of methionine residues of proteins: biological consequences. *Antioxid Redox Signal* **5**, 577–582.

Storm JF (1987). Action potential repolarization and a fast after-hyperpolarization in rat hippocampal pyramidal cells. *J Physiol* **385**, 733–759.

Sun H, Gao J, Ferrington DA, Biesiada H, Williams TD & Squier TC (1999). Repair of oxidized calmodulin by methionine sulfoxide reductase restores ability to activate the plasma membrane Ca-ATPase. *Biochemistry* **38**, 105–112.

Tang XD, Daggett H, Hanner M, Garcia ML, McManus OB, Brot N, Weissbach H, Heinemann SH & Hoshi T (2001). Oxidative regulation of large conductance calcium-activated potassium channels. *J General Physiol* **117**, 253–274.

Tang XD, Garcia ML, Heinemann SH & Hoshi T (2004). Reactive oxygen species impair Slo1 BK channel function by altering cysteine-mediated calcium sensing. *Nat Struct Mol Biol* **11**, 171–178.

Teh LC, Murphy LJ, Huq NL, Surus AS, Friesen HG, Lazarus L & Chapman GE (1987). Methionine oxidation in human growth hormone and human chorionic somatomammotropin. Effects on receptor binding and biological activities. *J Biol Chem* **262**, 6472–6477.

Tseng-Crank J, Foster CD, Krause JD, Mertz R, Godinot N, DiChiara TJ & Reinhart PH (1994). Cloning, expression, and distribution of functionally distinct Ca^{2+}-activated K^+ channel isoforms from human brain. *Neuron* **13**, 1315–1330.

Vogt W (1995). Oxidation of methionyl residues in proteins: tools, targets and reversal. *Free Radic Biol Med* **18**, 93–105.

Wallner M, Meera P & Toro L (1996). Determinant for beta-subunit regulation in high-conductance voltage-activated and Ca^{2+}-sensitive K^+ channels: an additional transmembrane region at the N terminus. *Proc Natl Acad Sci U S A* **93**, 14922–14927.

Weissbach H, Resnick L & Brot N (2005). Methionine sulfoxide reductases: history and cellular role in protecting against oxidative damage. *Biochim Biophys Acta* **1703**, 203–212.

Werner ME, Zvara P, Meredith AL, Aldrich RW & Nelson MT (2005). Erectile dysfunction in mice lacking the large-conductance calcium-activated potassium (BK) channel. *J Physiol* **567**, 545–556.

Xu W, Liu Y, Wang S, McDonald T, Van Eyk JE, Sidor A & O'Rourke B (2002). Cytoprotective role of Ca^{2+}-activated K^+ channels in the cardiac inner mitochondrial membrane. *Science* **298**, 1029–1033.

Zeng XH, Xia XM & Lingle CJ (2005). Divalent cation sensitivity of BK channel activation supports the existence of three distinct binding sites. *J General Physiol* **125**, 273–286.

Zhang L & McBain CJ (1995). Potassium conductances underlying repolarization and after-hyperpolarization in rat CA1 hippocampal interneurones. *J Physiol* **488**, 661–672.

Zhang X, Solaro CR & Lingle CJ (2001). Allosteric regulation of BK channel gating by Ca^{2+} and Mg^{2+} through a nonselective, low affinity divalent cation site. *J General Physiol* **118**, 607–635.

Zull JE, Smith SK & Wiltshire R (1990). Effect of methionine oxidation and deletion of amino-terminal residues on the conformation of parathyroid hormone. Circular dichroism studies. *J Biol Chem* **265**, 5671–5676.

Acknowledgements

We thank Drs R. Xu for cell culture and S. Hou for discussions. This work was supported in part by grants from the National Institutes of Health (T.H.) and the Interdisciplinary Center for Clinical Research and Thuringian Ministry for Science, Research, and Arts B307–04004 (S.H.H.).

Supplemental material

The online version of this paper can be accessed at:
DOI: 10.1113/jphysiol.2005.101089
http://jp.physoc.org/cgi/content/full/jphysiol.2005.101089/DC1
and contains supplemental material entitled:
Individual mutation of single methionine residues within hSlo1 does not remove the functional sensitivity to oxidation by Ch-T.

This material can also be found as part of the full-text HTML version available from http://www.blackwell-synergy.com